

**Reply to comments on “Impacts of Stratospheric Sulfate Geoengineering on Tropospheric Ozone” by Xia, Nowack, Tilmes and Robock, submitted to *Atmospheric Chemistry and Physics*.**

*Comments are repeated in black italics. Replies are indicated in blue.*

**Reviewer #1**

*General comments:*

*Different to the GeoMIP experiments G1 and G3, where greenhouse gas forcing is counteracted by balancing the top of the atmosphere (TOA) imbalance, the two techniques in this paper are balanced by the solar TOA forcing. However, they compare the results to Ferraro et al (2014) and Niemeier et al (2013) but these studies used the TOA imbalance. The paper is missing a discussion of this aspect. It might be an option to apply a bias correction, following Niemeier et al (2013). At least the discussion on precipitation should include the TOA energy balance and follow Liepert and Prevedi (2009) (see also Eq 8 in Niemeier et al 2013).*

Thanks for pointing that out. Niemeier et al. (2013) performed a FIX scenario, which freezes greenhouse gas concentrations. FIX is treated as an analog for a perfect compensation of the forcing through the greenhouse gas increase after 2020 and is unbiased by construction. They then bias corrected the mean net flux imbalance at TOA for three different SRM scenarios (sulfate injection, marine cloud brightening and solar reduction) to be the same as in FIX. After that correction, the global averaged surface temperature follows very similar trajectories in all scenarios. In our simulation, we keep the net solar flux at the TOA the same in G4SSA and G4SSA-S.

Although our experimental designs are different compared to Niemeier et al. (2013), we find that the resulting effects on the TOA fluxes are quite similar in G4SSA and G4SSA-S: the two geoengineering scenarios show similar TOA fluxes reduction (we have added Fig. S5 and Fig. 5a). Therefore, we think that bias correction is not needed, and differences in the hydrological cycle response are rather caused by differences in the model set-ups (ozone chemistry, lapse rate, evapotranspiration) as is already mentioned in the manuscript.

In order to highlight these differences in the experimental approach, the text in this section of the paper now reads (lines 197-230):

“The similar evaporation reduction in G4SSA and G4SSA-S can also be explained by the surface energy budget (Fig. 5b). Although we keep the net shortwave radiation at the TOA the same in the two schemes (Fig. 1a and Fig. 5a), surface net solar radiation reduces more in G4SSA than in G4SSA-S (Fig. 2c and Fig. 5b) due to the absorption by sulfate aerosols in the near-infrared. This stronger surface solar forcing in G4SSA-S is mainly balanced by larger net longwave radiation to the atmosphere (Fig. 5). As a result, latent heat changes in the two scenarios are similar.

Here, precipitation and evaporation changes are very similar under sulfate and solar geoengineering. This is different from previous studies by Niemeier et al. (2013) and Ferraro et al. (2014) who found that the effect on the hydrological cycle is larger for

sulfate geoengineering. These differences are related to the experimental design. Niemeier et al. (2013) bias corrected all geoengineering scenarios to keep the net total flux at the TOA the same as that in 2020, while we keep the same net solar flux at the TOA in G4SSA and G4SSA-S (Fig. 1a). However, we found the net total fluxes at the top of the model in G4SSA and G4SSA-S are similar as well (Fig. 5a and Fig. S5). Therefore, differences in the TOA boundary conditions might not be the main reason for the different hydrological cycle responses. In their studies, with the same magnitude of surface cooling, the sulfate injection scenario led to a greater reduction of globally averaged evaporation and precipitation as compared with the solar case. Ferraro et al. (2014) attributed the enhanced hydrological cycle response to sulfate geoengineering to extra downwelling longwave radiation because of stratospheric heating from the injected aerosols. Sulfate geoengineering thus led to a relative stabilization of the troposphere (by heating the upper troposphere more than the mid-lower troposphere) compared with the solar reduction case (which we do not find, Fig. 4c). A more stratified troposphere, in turn, results in a stronger reduction of latent heat fluxes and precipitation (similar to theoretical considerations by Bala et al. (2008)). We find two possible reasons for the different response in our experiments. (1) The column ozone change could play an important role. In Niemeier et al. (2013) and Ferraro et al. (2014), the same prescribed ozone was used in all scenarios, while we used a fully coupled atmosphere-chemistry model. As shown in section 3.2, total column ozone in G4SSA reduces by about 5 DU (mainly in the lower stratosphere) compared with RCP6.0 and G4SSA-S (Fig. 6). Less ozone in G4SSA will change its radiative forcing, surface radiative fluxes and atmospheric lapse rate (Chiodo and Polvani, 2015; MacIntosh et al., 2016; Nowack et al., 2015, 2017) and thus contribute to the differences between the two studies. (2) Enhanced transpiration in G4SSA due to enhanced diffuse radiation reduces the evaporation difference in the two SRM schemes as discussed above.”

*The naming of the experiments is sometimes confusing for the reader. Both SRM techniques start with S. G4SSA and G4SOL could be an alternative.*

Thanks, but we think G4SSA-S indicates solar reduction with the same forcing of G4SSA. G4SOL would be confused with solar reduction with the same forcing as G4.

*Specific Comments:*

*Line 119: The number of vertical levels is quite small compared to the horizontal resolution.*

Yes, this is CAM4-chem – a low top atmosphere model with fairly low vertical resolution. We understand the constraint of low vertical resolution, which might have an effect on the simulation of stratospheric dynamics. However, the representation of ozone in CAM4-chem has been evaluated and compares well to observations (Tilmes et al., 2016), as also shown in Fig. S1 and Fig. S2 in the supplement. In addition, the STE of ozone found here lies well within the range of typical model values in (high-top and high resolution) chemistry-climate models (Young et al., 2013). In future work, we plan to analyze output from a sulfate geoengineering simulation from the high top model WACCM to further investigate stratospheric dynamical changes with injected sulfate aerosols.

Young et al.: Pre-industrial to end 21<sup>st</sup> century projections of tropospheric ozone from the Atmospheric Chemistry and Climate Model Intercomparison Project (ACCMIP), *Atmos. Chem. Phys.*, 13, 2063-2090, doi:10.5194/acp-13-2063-2013, 2013.

*Line 128: Can you discuss the possible impact of the reduces solar radiation on the photolysis rate.*

Since the reviewer pointed the question is related to “Interaction between aerosol burden and photolysis rates is not included in the model”, we assume that the reviewer wants more details between the solar reduction due to aerosol and photolysis rate. We have added to the discussion in lines 137-142:

“Changes in photolysis rates in the troposphere depend on the stratospheric ozone column change (Kinnison et al., 2007). Increased ozone depletion as the result of geoengineering would therefore leads to an increase in UV in mid- and high latitudes. Since our model does not include the aerosol scattering effect on UV, expected UV reductions from the increased sulfate aerosol layer is not taken into account, which might result in an overestimation the tropospheric photolysis.”

*Line 169: This sentence is miss leading. It sounds like all references warm by 3 K.*

We have changed it in Lines 185-187:

“Sulfate aerosol in the stratosphere results in strong warming by 3 K in the tropics (Fig. 4a), while in G4SSA-S there is slight cooling (Fig. 4b), consistent with previous studies (Tilmes et sl., 2009; Ammann et al., 2010; Jones et al., 2011). ”

*Line 170: G4SSA-S shows also a slight warming in the lower stratosphere. Why?*

The slight warming in the lower stratosphere is probably a result of slightly increasing of ozone concentration in that regions and dynamical heating as the Brewer Dobson circulation slowing down (Fig. 8b). We have added in Lines 187-189:

“The slight warming in the lower stratosphere under G4SSA-S (Fig. 4b) might be a result of ozone changes and dynamical heating (discussion in Section 3.3.2).”

*Line 178 to 183: TOA imbalance as mentioned above. The difference between R-toa and R-surf are compensate by condensational heating. [1]Eq 1 in Niemeier et al (2013) was used for a bias correction. It might be an option to use this correction (G4SSA-S for I-FIX) to compensate the solar balancing but G4 has still a transient climate. However, it might be worth trying.*

In our simulation, we keep the net solar flux at the TOA the same in G4SSA and G4SSA-S, which results in the same net total fluxes change at the top of the model (Fig. S5 and Fig. 5a). Therefore, it is not necessary to bias correct the two scenarios as surface temperatures are also essentially identical (within expected limits). We have added text in the manuscript to highlight this. Please see our response to the general comment on page 1.

*Line 187: 'They attribute...' better 'Ferraro attribute ..' This was described earlier in a paper by Bala et al (2008).*

Bala et al. (2008) has been added. Changed.

*Line 222: Adding a row with differences in percent to the plot (Fig 7).*

We have added the differences in percentage as Fig. S7.

*Line 324: You say earlier that you do not change the photolysis rate. How is the reduced sunlight changing ozone here?*

In the section “Model and Experiment Design,” we mentioned that interactions between aerosol burden and photolysis rates are not included in the model and we have added more details (Lines 128-134). Changes in ozone will be triggered due to the changes in sunlight via (a) reduced ozone photolysis and (b) reduced oxygen photolysis that is needed for ozone production. Changes in stratospheric ozone in turn will affect tropospheric photolysis rates. However, overall such solar dimming effects will be small relative to other effects changing ozone (e.g., temperature and humidity) as the dimming in G4SSA-S is equivalent only to about 1% solar constant reduction.

*Line 356: This is not the only way to exchange ozone between stratosphere and troposphere. STE due to tropopause folds in the surf zone might be more important.*

Added in Lines 384-385:

“the rate of exchange of air masses between stratosphere and troposphere (i.e., the strength of the Brewer–Dobson (B-D) circulation and tropopause folds).”

*Line 383: Have you mentioned black carbon before?*

No, we didn't mention black carbon before. The only reason we put it here is stratospheric black carbon reduces tropospheric temperature and warms up stratosphere, similar to sulfate. And in those two studies, they showed a slow-down of tropical upwelling.

*Line 373 to 385: Your study uses a fixed QBO, different to Aquilla et al (2012). This may play an important role. Niemeier and Schmidt (2017) show also an increase in vertical velocity as well as a strong impact on stratospheric transport. This aspect cannot be taken into account in this study but might be discussed as a caveat.*

Thanks for pointing out that. Since Niemeier and Schmidt (2017) is currently ACPD, we will add this reference if it publishes before the publication of this manuscript. To strengthen the argument, we have added:

Lines 416-419:

“The differences between previous studies and our result may be because some previous studies used fixed ozone, with different stratospheric heating rates. In addition, in previous studies, the QBO was interactively simulated and the models had a higher model top.”

*Figures*

*May explanations in the text base on figures in the appendix. You may add them, or some of them, in the main text. It is easier for the reader and does not really matter in an online paper.*

The paper already has 10 figures, and there are 15 more in the supplemental. We feel that we present the research well already with the 10 figures, and adding a couple more would not make much difference. 10 figures is the traditional number of figures for a paper. The supplemental figures are for those interested in more details.

*Fig 2: Plot the ensemble mean as a running mean. This helps in recognizing differences or similarities.*

The ensemble means are already quite smooth curves, and a running mean would make it harder to see the changes at times of implementation and termination of geoengineering.

*Fig 4 and fig 8: It would be nice to see the position of the sulfate aerosol as a contour line.*

Done

*Fig 5: Add TOA energy fluxes*

Done

*Fig 6: Add additional years to the x-axis. Ozone decreases in RCP6 from roughly 2050, in G3SSA-S as well but not in G4SSA. Do you have an explanation?*

Axis changed. We are not sure which panel of Fig. 6 you refer to. In all the panels, the ozone depletion in the stratosphere in G4SSA is evident compared to the other two scenarios. The differences in surface ozone are explained in the paper.

*Fig 7: Add a row with differences in % (or use the figure from the appendix).*

Done. Figure added as Figure S7.

## **Reviewer #2**

*General comments:*

*On the whole, this paper is well-written except for a few places where clarification is needed.*

Thank you!

*For one, the description of the formulation of stratospheric chemistry in CAM-chem is missing.*

We have added in Lines 128-134:

“The tropospheric chemical mechanism in CAM4-chem is based on the Model for Ozone and Related chemical Tracers (MOZART), version 4 (Emmons et al., 2010). The stratospheric chemical mechanism is described in Kinnison et al. (2007), Lamarque et al. (2012) and Tilmes et al. (2015), and the complete chemical reactions included (photolysis, gas-phase chemistry and heterogeneous chemistry) are listed in Tilmes et al. (2016b), Table A2. Reaction rates are updated following Jet Propulsion Laboratory 2010 recommendations (Sander et al., 2011).”

*I was also wondering if the halogen loading and GHG concentrations all follow RCP 6.0 specifications such that the only differences between these three ensemble runs are sulfate aerosol loading for G4SSA and reduced solar fluxes for G4SSA-S.*

Yes, that is correct. In all scenarios (G4SSA, G4SSA-S and RCP6.0), the anthropogenic emissions follow the same pathway, and the only difference is the prescribed sulfate injection in G4SSA and the solar constant reduction in G4SSA-S. We have added a sentence to make this clear.

Lines 151-152: “Both geoengineering scenarios include RCP6.0 forcings.”

*Regardless, the time series of halogen loading should be given at some point in section 2. Citation of other research papers alone won't do for a broader readership.*

We have added in Lines 238-239:

“The halogen loading in the three scenarios is the same, and more information can be found in Morgenstern et al. (2017).”

The halogen loading is in Figure 1(b) of Morgenstern et al. (2017).

*Other minor points, (1) Lines 75-76: Please explain how emission pathways can determine transport from the ozone-rich stratosphere.*

Different emission pathways of halogens determine the recovery period of the ozone hole. The stratospheric ozone concentration will partially determine the ozone transported from stratosphere to troposphere. In addition, greenhouse gas emission pathways will result in different levels of global warming, which changes the stratospheric dynamics, such as the Brewer-Dobson circulation, and therefore alter the ozone transported from stratosphere to troposphere by different dynamics. Finally, different emission pathways (e.g. CO<sub>2</sub>, N<sub>2</sub>O and the resulting stratospheric water vapor feedback) will further change stratospheric background conditions (temperature, HOx,

NO<sub>x</sub>), with important consequences for stratospheric chemical reactions resulting in ozone production and depletion and thus, eventually, STE of ozone.

(2) Lines 304-305: Can you be more specific on how " the slow-down hydrological cycle under SRM will further enhance this tropospheric humidity reduction"?

We have deleted that sentence.

*Lastly for the geoengineering assessment to be practical, there needs to be a specific metric for measuring the impact. For example, the change in the distribution of tropospheric ozone in terms of the probability density distribution of surface ozone concentration might be useful.*

We agree that we need a specific metric for measuring the impact. We compared the geoengineering scheme with the reference case – RCP6.0. And we have done t-tests for each grid cell to understand whether the two scenarios are statistically different. In all maps, the hatched regions are insignificant, with  $p > 0.05$ .

*And the authors need to discuss what can be improved in the modeling effort in the discussion section.*

We have added sentences in Line 456-462:

“This study may be biased by the following factors: (1) using prescribed stratospheric aerosols does not allow the simulation of the full interactions between chemistry, aerosol microphysics, and dynamics. A fully interactive model including those interactions would be important. (2) The vertical resolution is not sufficient to produce an interactive QBO in the model used, which may also affect transport processes. (3) The model does not include the scattering effect of aerosols on tropospheric photolysis rates, which might lead to an overestimate of the UV enhancement in the troposphere.”

### **Reviewer #3**

*General comments:*

*This manuscript examined the effects of stratospheric sulfate aerosol and solar insolation reduction on tropospheric ozone and surface ozone. The study also examines the both chemical and transport mechanisms of tropospheric ozone changes to SRM techniques. The findings of this paper help us get a better understanding of effects of SRM. In general, I found the main points and the structure of this manuscripts are clear. Below are my comments for making the manuscript more concise. I recommended the paper to be published with minor revision.*

**Thanks.**

*Specific Comments:*

*Line 54: Add one or two references of sulfate aerosol effects in the stratosphere.*

Added in Lines 53-54:

“It is well known that sulfate aerosols in the stratosphere enhance heterogeneous chemical reactions that lead to enhanced ozone depletion after larger volcanic eruption (Solomon, 1999).”

*Caption for Figure S1: What do you mean about the 10N to 10S gridded present day MLS/OMI satellite data? Doesn't the data cover the extra-tropics?*

Zonal mean values from the satellite data were derived from a 10° x 10° gridded product. Model results were interpolated from the same grid.

*Line 159: move “the last 40 years of geoengineering” in line 161 to here.*

Changed.

*Line 163: Figure 3a and 3b: why there is significant temperature increase over north Atlantic? More explanations of temperature changes between SRM runs and RCP 6.0 would be helpful.*

We have added in Lines 178-180:

“The similar warming in the North Atlantic under G4SSA and G4SSA-S relative to RCP6.0 (Fig. 3a and 3b) is due to the regional cooling under RCP6.0 as a result of slowing down of the Gulf Stream (Hartmann et al., 2013).”

*Line 164-166: In Figure 3c: I did not see clear warming signal in Asia. And ‘warming’ here is confusing: both G4SSA and G4SSA-S show temperature decrease compared to RCP6.0. The red color in Figure 3c just means that G4SS4 has less temperature reduction than G4SS4-S.*

We have changed it to “The temperature difference between G4SSA and G4SSA-S (Fig. 3c) is larger in the Northern Hemisphere winter (Fig. S3).” (Lines 181-182)

*In Figure S3, surface temperature in G4SS4 does show a significant warming over northern Europe and Asia compared to RCP6.0 in winter. I think that is the feature that agrees with the characteristic “winter warming” from volcanic stratospheric aerosol (Robock, 2000).*

We have described this in Lines 182-184:

“The warming over northern Europe and Asia in G4SSA relative to G4SSA-S is the characteristic “winter warming” from volcanic stratospheric aerosol (Robock, 2000).”

*Line 168-170: around 50 hPa in the tropics, the G4SSA-S also shows the significant warming.*

The slight warming in the lower stratosphere might be a result of slight increases of ozone concentration there (Fig. 8b) and dynamic heating. We have added in Line 187-189:

“The slight warming in the lower stratosphere under G4SSA-S (Fig. 4b) is a result of ozone changes and dynamical heating (discussion in Session 3.3.2).”

*Line 173: would be better to switch the sequence of Figure 2b and Figure 2c*

Done

*Line 207: How the halogen changes over these three runs?*

We have added in Line 238-239:

“The halogen loading in the three scenarios is the same, and more information could be found in Morgenstern et al. (2017).”

The halogen loading is in Figure 1(b) of Morgenstern et al. (2017).

*Line 361: mid-high latitude: are you talking about the lower stratosphere  $\square$  100 hPa? Adding the location of tropopause in Figure 8 would be much helpful.*

Yes.

Instead of tropopause, we have added the prescribed sulfate aerosol layer as a contour line in Figure 8 as suggested by reviewer #1 on page 5. This might be better to help understanding the stratospheric warming and ozone depletion.

*Line 364: temperature changes in which direction?*

We have added in Line 393-394:

“changes in stratospheric temperature (warming in G4SSA and cooling in G4SSA-S) also change the photochemistry of ozone.”

*Line 364: “Altogether, this results in year-round lower stratospheric ozone loss world-wide that peaks during the return of sunlight at high SH latitudes.” Which figure describes this feature?*

We have added Fig. S14

*Line 368: Figure 8b: Confused here: in Figure 4b, temperature shows an increase in the tropics around 50-70 hPa. Other regions show temperature reduction. You mentioned that ozone increase in Figure 8b is due to temperature decreases. While the regions with T increases (tropics, 50-70 hPa), ozone has a maximum increase.*

The slight warming in the lower stratosphere in Fig. 4b might be a result of slight increases of ozone concentration there (Fig. 8b). We have added in Lines 187-189:

“The slight warming in the lower stratosphere under G4SSA-S (Fig. 4b) is a result of ozone changes and dynamic heating (discussion in Section 3.3.2).”

We have added discussion in 3.3.2 line 399-404:

“However, in Fig. 4b, there is a slight warming around 50 mb in the tropics, where ozone concentration also shows a stronger increase (Fig. 8b). As tropospheric cooling results in a slow-down of the B-D circulation (Fig. 9b) (Lin and Fu, 2013; Nowack et al., 2015; Shepherd and McLandress, 2011), there is an increase of ozone in the tropical upwelling region, which leads to increasing temperatures there as ozone is a strong shortwave and longwave absorber.”

*It would be much easier to understand if you mention lat/pressure when describing figures. Lower stratosphere in the polar region could reach as low as 400 hPa. Adding a tropopause in Figure 8 would be much helpful.*

We have added the latitude and the altitude in lines 390 and 392. We have added the injected sulfate aerosol as contour lines in Figure 8.

*Line 383-384: Why tropical upwelling response differently between this study and Aquila et al 2012? Please be more specific?*

We have added in Lines 416-419:

“The differences between previous studies and our result may be because some previous studies used fixed ozone, with different stratospheric heating rates. In addition, in previous studies, the QBO was interactively simulated and the models had a higher model top.”

*Line 394: (Fig. S12). . delete one period*

Done.

1           **Impacts of Stratospheric Sulfate Geoengineering on Tropospheric Ozone**

2           Lili Xia<sup>1\*</sup>, Peer J. Nowack<sup>2</sup>, Simone Tilmes<sup>3</sup>, and Alan Robock<sup>1</sup>

3           <sup>1</sup>Department of Environmental Sciences, Rutgers University, New Brunswick, New Jersey, USA

4           <sup>2</sup>Centre for Atmospheric Science, Department of Chemistry, University of Cambridge,  
5           Cambridge, UK

6           [Now at Imperial College London, Grantham Institute and Department of Physics, Faculty of](#)  
7           [Natural Sciences, London, UK](#)

8           <sup>3</sup>Atmospheric Chemistry Division, National Center of Atmospheric Research, Boulder, CO, USA

9  
10           Submitted to *Atmospheric Chemistry and Physics*

          Special Issue: Geoengineering Model Intercomparison Project

11                           ~~May~~August 2017

12  
13  
14  
15  
16  
17  
18  
19  
20  
21  
22  
23  
24  
\*To whom correspondence should be addressed: Lili Xia, Department of Environmental Sciences,  
Rutgers University, 14 College Farm Road, New Brunswick, NJ 08901-8551. E-mail:  
lxia@envsci.rutgers.edu.

26

### Abstract

27 A range of solar radiation management (SRM) techniques has been proposed to counter  
28 anthropogenic climate change. Here, we examine the potential effects of stratospheric sulfate  
29 ~~aerosol~~aerosols and solar insolation reduction on tropospheric ozone and ozone at Earth's surface.  
30 Ozone is a key air pollutant, which can produce respiratory diseases and crop damage. Using a  
31 version of the Community Earth System Model from the National Center for Atmospheric  
32 Research that includes comprehensive tropospheric and stratospheric chemistry, we model both  
33 stratospheric sulfur injection and solar irradiance reduction schemes, with the aim of achieving  
34 equal levels of surface cooling relative to the Representative Concentration Pathway 6.0 scenario.  
35 This allows us to compare the impacts of sulfate ~~aerosol~~aerosols and solar dimming on  
36 atmospheric ozone concentrations. Despite nearly identical global mean surface temperatures for  
37 the two SRM approaches, solar insolation reduction increases global average surface ozone  
38 concentrations while sulfate injection decreases it. A key fundamental difference between the two  
39 geoengineering schemes is the importance of heterogeneous reactions in the photochemical ozone  
40 balance with larger stratospheric sulfate abundance, resulting in increased ozone depletion in mid-  
41 and high latitudes. This reduces the net transport of stratospheric ozone into the troposphere and  
42 thus is a key driver of the overall decrease in surface ozone. At the same time, the change in  
43 stratospheric ozone alters the tropospheric photochemical environment due to enhanced ultraviolet  
44 radiation. A shared factor among both SRM scenarios is decreased chemical ozone loss due to  
45 reduced tropospheric humidity. Under insolation reduction, this is the dominant factor giving rise  
46 to the global surface ozone increase. Regionally, both surface ozone increases and decreases are  
47 found for both scenarios, that is, SRM would affect regions of the world differently in terms of air  
48 pollution. In conclusion, surface ozone and tropospheric chemistry would likely be affected by  
49 SRM, but the overall effect is strongly dependent on the SRM scheme. Due to the health and  
50 economic impacts of surface ozone, all these impacts should be taken into account in evaluations  
51 of possible consequences of SRM.

52

Formatted: Line spacing: At least 24 pt

53 **1 Introduction**

54 **1.1 Atmospheric Ozone**

55 It is well known that sulfate aerosols in the stratosphere enhance heterogeneous chemical  
56 reactions that lead to enhanced ozone depletion- after larger volcanic eruptions (Solomon, 1999).  
57 With present day anthropogenic halogen loading, the aerosols provide additional surface area for  
58 heterogeneous reactions that activate halogens and hence increase catalytic ozone destruction,  
59 especially in high latitudes (Tie and Brasseur, 1995). This has been modeled and observed  
60 following the large 1982 El Chichón and 1991 Pinatubo volcanic eruptions (Tie and Brasseur,  
61 1995; Portman et al., 1996; ~~Solomon, 1999~~).

62 However, volcanic eruptions do not only affect stratospheric ozone, but also impact  
63 tropospheric composition, often due to stratosphere-troposphere coupled effects. The 1991  
64 Pinatubo eruption, for example, has been linked to changes in stratosphere-troposphere exchange  
65 (STE) of ozone (Aquila et al., 2012; Aquila et al., 2013; Pitari et al., 2016). In addition, the  
66 stratospheric ozone decrease led to an invigorated photochemical environment in the troposphere  
67 due to enhanced downward chemically-active ultraviolet (UV) radiation (Tang et al., 2013).

68 This study focuses on tropospheric ozone, in particular surface ozone concentration  
69 changes. Surface ozone is of central importance to Earth's environment and as an air pollutant it  
70 adversely impacts human health (e.g., Kampa and Castanas, 2008) and the ecosystem (e.g.,  
71 Mauzeral and Wang, 2001; Ashmore, 2005; Ainsworth et al., 2012). There have been numerous  
72 studies of the observed surface ozone trend (e.g., Cooper et al., 2014), identifying ozone sources  
73 and sinks (e.g., Wild, 2007), predicting future changes (e.g., Young et al., 2013), and  
74 understanding the impacts of such changes (e.g., Silva et al., 2013). Global surface ozone  
75 concentrations are estimated to have doubled since the preindustrial period (Vingarzan, 2004),

76 mainly due to increased emissions of ozone precursors associated with industrialization (e.g.,  
77 Forster et al., 2007). Differences in future tropospheric ozone concentrations will be strongly  
78 dependent on the emission pathway followed (Stevenson et al., 2006), which will determine both  
79 in-situ tropospheric chemical production of ozone and transport from the ozone-rich stratosphere  
80 (Collins et al., 2003; Wild et al., 2012; Neu et al., 2014).

### 81 **1.2 Differences between sulfate and solar geoengineering**

82 The progression of global warming, slow mitigation efforts, and our relatively limited  
83 adaptive capacity, force consideration of SRM geoengineering as one possible strategy to avoid  
84 many of the most undesirable consequences of global warming (Crutzen, 2006; Wigley, 2006;  
85 Tilmes, 2016a). The above discussed factors controlling tropospheric ozone concentrations could  
86 be affected by SRM schemes (Nowack et al., 2016). Here we compare a proposed geoengineering  
87 scheme, stratospheric sulfur injection, to solar irradiance reduction. Both schemes would cool  
88 Earth's surface by reducing sunlight reaching the surface, either by aerosols reflecting sunlight or  
89 by artificially reducing the solar constant in a climate model, but sulfate geoengineering would  
90 strongly heat the stratosphere and provide aerosol surfaces for chemical reactions. Previous  
91 studies have shown that injected sulfur chemically forms sulfate aerosols within a couple of weeks.  
92 The aerosol layer absorbs near infrared solar radiation as well as outgoing longwave radiation and  
93 results in stratospheric warming (e.g., Tilmes et al., 2009; Ammann et al., 2010; Jones et al., 2011).  
94 Additionally changes in ozone and advection impact the warming in the stratosphere (Richter et  
95 al., 2017, submitted). Under solar reduction, the stratosphere would be cooler due to reduced  
96 shortwave heating (Govindasamy and Caldeira, 2000), although simultaneous stratospheric ozone  
97 changes (if considered) may buffer this effect (Nowack et al., 2016).

98 One of the most important differences between the two scenarios is that if a permanently  
99 enhanced stratospheric aerosol layer is artificially created in an attempt to reduce anthropogenic  
100 global warming, the resulting strong ozone depletion, in particular in mid- and high latitudes,  
101 would have serious impacts on the biosphere, similar to the effects observed after large volcanic  
102 eruptions described above (Crutzen, 2006; Rasch et al., 2008a; Rasch et al., 2008b; Tilmes et al.,  
103 2008, 2009, 2012). This effect would have to be expected as long as there is anthropogenic halogen  
104 in the stratosphere. In the remote future, the decreasing burden of anthropogenic halogen  
105 ~~components~~ will eventually result in an increase in the recovery of the ozone layer. Under such  
106 conditions additional stratospheric ~~ozone due to the importance of heterogeneous reactions to the~~  
107 ~~nitrogen cycle in aerosols could actually have~~ the ~~upper stratosphere, which increases~~ opposite  
108 effect by deactivating ozone depleting nitrogen oxides, thus leading to an increase in ozone in the  
109 ~~middle and upper~~ stratosphere (Tie and Brasseur, 1995; Pitari et al, 2014). Overall, such changes  
110 to the stratosphere would also have important implications for tropospheric composition.  
111 Decreasing stratospheric ozone leads to more UV propagating through, with increasing ozone  
112 having the opposite effect, which would thus alter the photochemical environment of the  
113 troposphere in different ways (Tilmes et al., 2012; Nowack et al., 2016).

114 In the following sections, we describe the experimental set-up of the two geoengineering  
115 schemes and discuss some general climate impacts, followed by a detailed discussion of  
116 tropospheric and surface ozone changes. We also show that sulfate and solar geoengineering  
117 would impact the stratosphere differently, which implies further key differences in their potential  
118 influences on tropospheric composition. In this study, we examine the impacts of stratospheric  
119 sulfate geoengineering on tropospheric ozone for the first time.

120 **2 Model and Experiment Design**

121 We simulated both types of SRM schemes using the full tropospheric and stratospheric  
122 chemistry version of the Community Earth System Model – Community Atmospheric Model 4  
123 (CESM CAM4-chem) with horizontal resolution of 0.9° x 1.25° lat-lon and 26 levels from the  
124 surface to about 40 km (3.5 mb). The model has been shown to give a good representation of  
125 present-day atmospheric composition in the troposphere (Tilmes et al., 2016b) and stratosphere at  
126 2° resolution (Fernandez et al., 2017). Similar to the 2° model version, the 1° horizontal resolution  
127 version of the model also produces reasonable stratosphere and troposphere ozone chemistry (Figs.  
128 S1-S2). CAM4-chem is fully coupled to the Community Land Model version 4.0 with prescribed  
129 satellite phenology (CLM4SP), the Parallel Ocean Program version 2 (POP2) ocean model ~~and the~~  
130 ~~Los Alamos sea ice model (CICE version 4).~~ and the Los Alamos sea ice model (CICE version  
131 4). The tropospheric chemical mechanism in CAM4-chem is based on the Model for Ozone and  
132 Related chemical Tracers (MOZART) version 4 (Emmons et al., 2010). The stratospheric  
133 chemical mechanism is described in Kinnison et al. (2007), Lamarque et al. (2012) and Tilmes et  
134 al. (2015), and the complete chemical reactions included (photolysis, gas-phase chemistry and  
135 heterogeneous chemistry) are listed in Tilmes et al. (2016b), Table A2. Reaction rates are updated  
136 following Jet Propulsion Laboratory 2010 recommendations (Sander et al., 2011). The model uses  
137 a nudged quasi-biennial oscillation (QBO), which means the QBO will not be modified by the  
138 radiative interaction of the ~~aerosols~~ aerosols. Interaction between aerosol burden and photolysis  
139 rates is not included in the model. Changes in photolysis rates in the troposphere ~~are calculated~~  
140 ~~depending on the total ozone column change (Kinnison et al., 2007).~~ depend on the stratospheric  
141 ozone column change (Kinnison et al., 2007). Increased ozone depletion as the result of  
142 geoengineering would therefore leads to an increase in UV in mid- and high latitudes. Since our

Formatted: Keep with next

Formatted: Normal, Don't adjust right indent when grid is defined, No widow/orphan control, Don't adjust space between Latin and Asian text, Don't adjust space between Asian text and numbers

Formatted: Font color: Black

143 model does not include the aerosol scattering effect on UV, expected UV reductions from the  
144 increased sulfate aerosol layer is not taken into account, which might result in an overestimation  
145 of the tropospheric photolysis. Volatile organic compound (VOC) emissions are simulated by the  
146 Model of Emission of Gases and Aerosols from Nature (MEGAN v2.1) (Guenther et al., 2012).  
147 The dynamical ocean model does not include any biogeochemical feedbacks and only the  
148 atmospheric and land models are coupled to the atmospheric chemistry component. The model  
149 configuration used here, but at 2° resolution, is participating in the current phase of the Chemistry-  
150 Climate Model Initiative (Tilmes et al., 2016b, Morgenstern et al., 2017).

151 We compare three ensemble members each of the two geoengineering scenarios to a three-  
152 ensemble reference run with Representative Concentration Pathway 6.0 (RCP6.0; Meinshausen et  
153 al., 2011) anthropogenic forcing from 2020 to 2089. Both geoengineering scenarios include  
154 RCP6.0 forcings. Our sulfate aerosol implementation is the G4 Specified Stratospheric Aerosol  
155 (G4SSA) experiment (Tilmes et al., 2015), whereas solar reduction geoengineering is the solar  
156 analog (hereafter G4SSA-S) by imposing a solar irradiance reduction with the same negative  
157 radiative forcing at the top of the atmosphere (TOA) as in G4SSA. G4SSA uses a prescribed  
158 stratospheric aerosol surface area distribution to mimic the effects of continuous emission into the  
159 tropical stratosphere at 60 mb of 8 Tg SO<sub>2</sub> yr<sup>-1</sup> from 2020 to 2069. More details of this prescribed  
160 stratospheric aerosol distribution are given in Tilmes et al. (2015b) and Xia et al. (2016). The  
161 G4SSA scenario then continues from 2070 to 2089 without imposed aerosols to study the  
162 termination effect of geoengineering. During the sulfate injection period, the net solar flux at the  
163 TOA has been decreased by 2.5 W/m<sup>2</sup> compared to RCP6.0 (Fig. 1a). This number was obtained  
164 by a double radiation call in the model in calculating the direct forcing of the prescribed aerosol  
165 layer. To attain the same TOA solar flux reduction in G4SSA-S, we reduced the total solar

Formatted: Font: Times, Font color: Black

166 insolation by  $14.7 \text{ W/m}^2$  during 2020-2069 assuming a global average planetary albedo of 0.32  
167 ( $14.7 \text{ W/m}^2 = \frac{2.5 \text{ W/m}^2 \times 4}{1.0 - 0.32}$ ) (Fig. 1b). From 2070 on, we accordingly reset the total solar  
168 insolation back to the reference level to simulate the abrupt termination of geoengineering.

### 169 3 Results and Discussion

#### 170 3.1 Climatology in G4SSA and G4SSA-S

171 As a consequence of the same net all-sky TOA solar flux reduction in G4SSA and G4SSA-  
172 S (Fig. 1a), the two scenarios show approximately the same global mean surface temperature  
173 reduction of 0.8 K compared with RCP6.0 (Fig. 2a) (all values below are the average of years  
174 2030-2069, the last 40 years of geoengineering). After the termination of geoengineering on 1  
175 January 2070, the global mean surface temperature rapidly increases. Fig. 3 shows the surface  
176 temperature differences between G4SSA, G4SSA-S, and RCP6.0 in years 2030-2069 ~~(the last 40~~  
177 ~~years of geoengineering)~~. Consistent with the global average temperature change, the two  
178 geoengineering scenarios have similar temperature reduction patterns (Fig. 3a and 3b), and the  
179 differences between them are not significant in most regions (Fig. 3c). The similar warming in  
180 northern Europe and Asia shown in the North Atlantic under G4SSA and G4SSA-S relative to  
181 RCP6.0 (Fig. 3a and 3b) is stronger due to the regional cooling under RCP6.0 as a result of  
182 slowing down of the Gulf Stream (Hartmann et al., 2013). The temperature difference between  
183 G4SSA and G4SSA-S (Fig. 3c) is larger in the Northern Hemisphere winter (Fig. S3), which  
184 The warming over northern Europe and Asia in G4SSA relative to G4SSA-S is the characteristic  
185 “winter warming” from volcanic stratospheric ~~aerosol~~aerosols (Robock, 2000). However, the  
186 zonal mean stratospheric temperatures in G4SSA and G4SSA-S differ substantially (Fig. 4). ~~As~~  
187 ~~shown in~~Sulfate aerosols previous studies (Tilmes et al., 2009; Ammann et al., 2010; Jones et al.,  
188 2011), sulfate aerosol in the stratosphere ~~results~~result in strong warming by 3 K in the tropics (Fig.

189 4a), while in G4SSA-S there is slight cooling (Fig. 4b), consistent with previous studies (Tilmes  
190 et al., 2009; Ammann et al., 2010; Jones et al., 4b)-2011). The slight warming in the lower  
191 stratosphere under G4SSA-S (Fig. 4b) might be a result of ozone changes and dynamical heating  
192 (discussion in Section 3.3.2). In both cases, the troposphere shows strong temperature reduction  
193 with similar patterns and ranges.

194 Global averaged precipitation and evaporation have similar ~~size~~ reductions of 0.07 mm/day  
195 in the two scenarios (Fig. 2e2b and Fig. S4), with no statistically significant difference between  
196 them. Most of the evaporation terms show a larger reduction in G4SSA than in G4SSA-S, except  
197 for plant transpiration, which has the opposite pattern (Fig. S4). As shown by Xia et al. (2016),  
198 enhanced diffuse radiation in G4SSA increases photosynthesis, which produces stronger  
199 transpiration. Therefore, transpiration in G4SSA reduces less than in G4SSA-S.

200 The similar evaporation reduction in G4SSA and G4SSA-S can also be explained by the  
201 surface energy budget (Fig. 55b). Although we keep the net shortwave radiation at the TOA the  
202 same in the two schemes (Fig. 1a and Fig. 5a), surface net solar radiation reduces more in G4SSA  
203 than in G4SSA-S (Fig. 2b2c and Fig. 55b) due to the absorption by sulfate aerosols in the  
204 near-infrared. This stronger surface solar forcing in G4SSA-S is mainly balanced by larger net  
205 longwave radiation to the atmosphere (Fig. 5). As a result, latent heat changes in the two scenarios  
206 are similar.

207 ~~The~~Here, precipitation and evaporation changes ~~in this study are~~ are very similar under  
208 sulfate and solar geoengineering. This is different from previous studies by Niemeier et al. (2013)  
209 and Ferraro et al. (2014-) who found that the effect on the hydrological cycle is larger for sulfate  
210 geoengineering. These differences are related to the experimental design. Niemeier et al. (2013)  
211 bias corrected all geoengineering scenarios to keep the net total flux at the TOA the same as that

212 in 2020, while we keep the same net solar flux at the TOA in G4SSA and G4SSA-S (Fig. 1a).  
213 However, we found the net total fluxes at the top of the model in G4SSA and G4SSA-S are similar  
214 as well (Fig. 5a and Fig. S5). Therefore, differences in the TOA boundary conditions might not  
215 be the main reason for the different hydrological cycle responses. In their studies, with the same  
216 magnitude of surface cooling, the sulfate injection scenario led to a greater reduction of globally  
217 averaged evaporation and precipitation as compared with the solar case. ~~They attribute this~~  
218 ~~result~~ Ferraro et al. (2014) attributed the enhanced hydrological cycle response to sulfate  
219 geoengineering to extra downwelling longwave radiation because of stratospheric heating from  
220 the injected aerosol, which would heat aerosols. Sulfate geoengineering thus led to a relative  
221 stabilization of the troposphere (by heating the upper troposphere and stabilize more than the mid-  
222 lower troposphere) compared with the solar reduction case (which we did not find, Fig. 4c), and  
223 result). A more stratified troposphere, in turn, results in a stronger reduction of latent heat fluxes  
224 and precipitation in sulfate injection geoengineering (similar to theoretical considerations by Bala  
225 et al. (2008)). We find two possible reasons for the differences: different response in our  
226 experiments. (1) The column ozone change ~~plays~~ could play an important role. In Niemeier et al.  
227 (2013) and Ferraro et al. (2014), the same prescribed ozone was used in all scenarios, while we  
228 used a fully coupled atmosphere-chemistry model. As shown in section 3.2, total column ozone  
229 in G4SSA reduces by about 5 DU (mainly in the lower stratosphere) compared with RCP6.0 and  
230 G4SSA-S (Fig. 6). Less ozone in G4SSA will change its radiative forcing, surface radiative fluxes  
231 and atmospheric lapse rate (Chiodo and Polvani, 2015; MacIntosh et al., 2016; Nowack et al., 2015,  
232 2017) and thus contribute to the differences between the two studies. (2) Enhanced transpiration  
233 in G4SSA due to enhanced diffuse radiation reduces the evaporation difference in the two SRM  
234 schemes as discussed above.

### 235 3.2 Surface and tropospheric ozone response

236 The ozone response is remarkably different in G4SSA and G4SSA-S. Global mean surface  
237 ozone increases under G4SSA-S and decreases under G4SSA, relative to RCP6.0 (Fig. 6a). The  
238 total ozone column is dominated by stratospheric column ozone, and shows strong reduction under  
239 G4SSA compared to RCP6.0, while the increase under G4SSA-S is small (Figs. 6b and 6d). The  
240 underlying upward trends of total column ozone as well as stratospheric ozone in all three scenarios  
241 are in line with the gradually declining stratospheric halogen content over time (Figs. 6b and 6d).

242 The halogen loading in the three scenarios is the same, and more information can be found in  
243 Morgenstern et al. (2017). As there is less halogen in the stratosphere ~~toward~~toward the end of  
244 the geoengineering, stratospheric ozone is recovering (Fig. 6d) and there is less reduction of the  
245 total ozone column in G4SSA relative to RCP6.0 (Fig. 6b). The agreement ~~of all curves as~~  
246 concerns across the simulations concerning interannual and decadal variations is because of the  
247 imposed QBO and 11-year solar cycles in all the runs. The decreasing tropospheric ozone column  
248 and surface ozone after year 2060 in all scenarios results from ~~the decreases in~~ global ozone  
249 precursor emissions ~~decrease~~ following the RCP6.0 scenario (Young et al., 2013).

250 The surface ozone concentration distributions in the three scenarios are similar, with the  
251 highest concentration over the continents in the Northern Hemisphere (NH) (Fig. ~~S5S6~~), while the  
252 concentration differences as well as the percentage difference between scenarios are spatially  
253 variable (Fig. 7 and Fig. S7). This highlights that the key driver behind the absolute surface ozone  
254 abundances is the underlying ozone precursor emissions following the RCP6.0 scenario. SRM is  
255 only a modulating factor, but depending on the SRM scheme even the sign of its impact can differ;  
256 global mean surface ozone concentrations in G4SSA are lower, relative to RCP6.0, whereas there  
257 are ~~mild~~moderate surface ozone increases over the tropics (Fig. 7a). The strongest surface ozone

258 reductions compared with RCP6.0 occur in NH mid-latitudes across all seasons (Figs. ~~S6aS8a-d~~)  
259 and Southern Hemisphere (SH) mid-to-high latitudes in MAM and JJA (Figs. ~~S6bS8b, c~~). ~~As~~  
260 ~~discussed in the next section, the reduction over the continents is related to atmospheric chemistry~~  
261 ~~changes while the reduction over the polar regions in the winter hemisphere is due to transport.~~ In  
262 G4SSA-S, surface ozone also increases in the tropics relative to RCP6.0 (Fig. 7b), and this regional  
263 change is greater than in G4SSA (Fig. 7c). Surface ozone decreases, however, are found at NH  
264 mid-latitudes over the continents during all seasons (Fig. ~~S6eS8e-h~~). Comparing the two types of  
265 geoengineering experiments directly, surface ozone concentrations are generally lower in G4SSA  
266 than in G4SSA-S (Fig. 7c), with peak differences in terms of absolute changes (ppb) at SH mid-  
267 to-high latitudes in MAM and JJA (Fig. ~~S6iS8i, j~~) and at NH mid-to-high latitudes in DJF (Fig.  
268 ~~S6iS8i~~).

### 269 3.3 Mechanisms of surface ozone change

270 Surface ozone concentrations are determined by chemical production and loss controlled  
271 by emissions of ozone precursors and the composition of the atmosphere, loss due to surface  
272 deposition of ozone, and ~~the~~ transport of ozone from other regions of the atmosphere (Monks et  
273 al., 2015). Since all scenarios considered here are based on the same RCP6.0 emission scenario  
274 of ozone precursors, such as nitrogen oxide (NO<sub>x</sub>) and methane (CH<sub>4</sub>), the differences in surface  
275 ozone must necessarily be driven by changes in climate in response to the geoengineering  
276 interventions, which include changes in temperature, humidity, atmospheric dynamics, and the  
277 photochemical environment. To understand the differences mechanistically, it is helpful to  
278 consider the impact of geoengineering on the tropospheric ozone budget.

279 The upper part of Table 1 shows the sources (production and net transport from the  
280 stratosphere (stratosphere-troposphere-exchange, STE)) and sinks (loss rates and dry deposition)

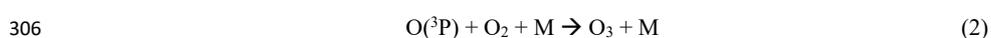
281 of tropospheric ozone. Both G4SSA and G4SSA-S show positive net chemical change of  
282 tropospheric ozone (chemical production minus loss) and negative change in STE of ozone relative  
283 to RCP6.0. However, the magnitude of these changes is significantly different. Compared with  
284 RCP6.0, tropospheric ozone net chemical change increases by  $\sim 125 \text{ Tg yr}^{-1}$  and  $\sim 40 \text{ Tg yr}^{-1}$  in  
285 G4SSA and G4SSA-S, respectively, whereas STE of ozone decreases by  $\sim 140 \text{ Tg yr}^{-1}$  ( $\sim 25\%$ ) and  
286  $\sim 30 \text{ Tg yr}^{-1}$  ( $\sim 5\%$ ) in G4SSA and G4SSA-S, respectively. The positive net chemical changes are  
287 the result of reductions in both chemical ozone production and loss under G4SSA and G4SSA-S  
288 relative to RCP6.0, with larger reductions in ozone loss reactions (Table 1). Specifically, G4SSA-  
289 S shows a  $\sim 90 \text{ Tg yr}^{-1}$  larger decrease in ozone chemical production, whereas ozone loss budgets  
290 are reduced by similar magnitudes for the two SRM schemes ( $262.5 \text{ Tg yr}^{-1}$  and  $269.5 \text{ Tg yr}^{-1}$ ).  
291 Combining the chemical and transport changes, the tropospheric ozone budget decreases under  
292 G4SSA and increases under G4SSA-S relative to RCP6.0, which is consistent with the overall  
293 surface ozone changes.

294 The reasons for these specific changes are discussed in detail in the following two sections.  
295 Then, the impacts of the factors are combined to explain regional surface ozone differences, as  
296 shown in Fig. 7.

### 297 **3.3.1 Chemical ozone production and loss in the troposphere**

298 Changes in tropospheric water vapor concentrations and the tropospheric photolysis  
299 environment under G4SSA and G4SSA-S are key to understand the differences in tropospheric  
300 ozone production and loss. This result is consistent with results of a previous study for the case of  
301 solar geoengineering under a more idealized forcing scenario (Nowack et al., 2016).

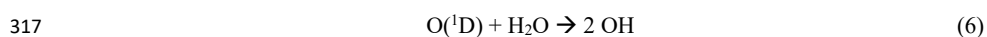
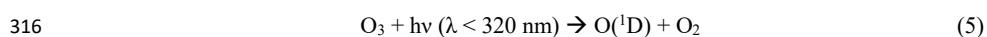
302 To explain this, we briefly re-iterate that tropospheric ozone (O<sub>3</sub>) production is driven by  
303 photolysis of nitrogen dioxide (NO<sub>2</sub>) and the subsequent formation of ozone via a three-body-  
304 reaction with resulting ground state atomic oxygen O(<sup>3</sup>P) (Monks, 2005),



307 where M is an inert collision partner (mostly molecular nitrogen). NO<sub>2</sub> formation in turn is  
308 crucially dependent on the oxidation of NO by reaction with peroxides present in the troposphere,  
309 for example,



312 where R represents general organic residues such as CH<sub>3</sub> (row 6 in Table 1). RO<sub>2</sub> in turn is  
313 produced by oxidation reactions between VOCs and the hydroxyl radical OH. Tropospheric OH  
314 is formed primarily by ozone photolysis and subsequent reaction of excited atomic oxygen O(<sup>1</sup>D)  
315 with water vapor,



318 Reaction (6) competes with several other reactions due to the high reactivity of O(<sup>1</sup>D). However,  
319 most importantly, the majority of O(<sup>1</sup>D) is quenched by collision with inert molecules such as  
320 molecular nitrogen to ground state atomic oxygen O(<sup>3</sup>P), which subsequently undergoes  
321 reformation to O<sub>3</sub> via three-body-reaction (2). Therefore, tropospheric ozone production and loss  
322 is strongly linked to concentrations of water vapor and the photochemical environment  
323 (availability of UV) in the troposphere.

324 In the case of clean (low  $\text{NO}_x$ ) environments, lower water vapor concentrations (mainly in  
325 the tropical region  $30^\circ\text{N} - 30^\circ\text{S}$ ) (Fig. [S7S9](#)) lead to less ozone loss via reactions (5) and (6) and  
326 additional reactions with the formed HOx species ( $\text{r-O}(^1\text{D})\text{-H}_2\text{O}$ ,  $\text{r-OH-O}_3$ , and  $\text{r-HO}_2\text{-O}_3$  in Table  
327 1). This happens at the expense of more quenching of  $\text{O}(^1\text{D})$  and subsequent recycling of ozone,  
328 thus resulting in ozone increases. In contrast, in polluted (high  $\text{NO}_x$ ) environments, less OH  
329 formation under lower atmospheric water vapor concentrations leads to reduced formation of  $\text{RO}_2$   
330 and  $\text{HO}_2$ . Therefore, less  $\text{NO}_2$  is produced via reactions (3) and (4), resulting in less catalytic  
331 ozone production via reactions (1) and (2) ( $\text{r-NO-HO}_2$  and e.g.  $\text{r-CH}_3\text{O}_2\text{-NO}$  in Table 1).  
332 Consequently, ozone production is reduced in  $\text{NO}_x$ -polluted environments under lower  
333 atmospheric water vapor concentrations.

334 With these fundamentals in mind, it is possible to understand the sign of the tropospheric  
335 ozone loss and production rate changes summarized in Table 1. Under both G4SSA and G4SSA-  
336 S, the key objective is to achieve surface temperature decreases. Tropospheric water vapor  
337 concentrations (or specific humidity) are strongly coupled to surface temperatures, because  
338 relative humidity does not change much with climate change (Soden and Held, 2006; Dessler and  
339 Sherwood, 2009), so that the surface cooling simultaneously reduces tropospheric specific  
340 humidity by 5-20% depending on region and altitude. ~~The slow down of the hydrological cycle  
341 under SRM will further enhance this tropospheric humidity reduction (Bala et al., 2002; Tilmes et  
342 al., 2013; Nowack et al., 2016).~~ As a result, less water vapor in both G4SSA and G4SSA-S reduces  
343 ozone chemical loss by  $\sim 150 \text{ Tg yr}^{-1}$  through reactions (5) and (6). The resulting decrease in  $\text{HO}_x$   
344 leads to further reductions in ozone loss, i.e., via reaction with OH ( $\sim 20 \text{ Tg yr}^{-1}$ ) and  $\text{HO}_2$  ( $\sim 60\text{-}70$   
345  $\text{ Tg yr}^{-1}$ ). Overall, these water vapor/ $\text{HO}_x$ -related reactions explain  $\sim 90\%$  of the overall reduction  
346 in ozone loss under SRM compared to a future RCP6.0 simulation.

347 The reduction in atmospheric humidity also affects ozone production, but to a smaller  
348 degree. Here, ozone production via reaction between NO and HO<sub>2</sub> is the key factor in driving  
349 these changes, with reductions of ~55 and 120 Tg yr<sup>-1</sup> for G4SSA and G4SSA-S, respectively.  
350 The signal of reduced OH production propagates through all other NO<sub>x</sub>-catalyzed ozone  
351 production pathways involving RO<sub>2</sub> via reactions (4) and subsequently (1) and (2). NO oxidation  
352 via the CH<sub>3</sub>O<sub>2</sub>-NO pathway decreases by ~27 and 49 Tg yr<sup>-1</sup> in G4SSA and G4SSA-S. Changes  
353 in natural NO<sub>x</sub> emissions by lightning play a minor role in comparison. In both SRM schemes,  
354 the reduction of lightning induced NO<sub>x</sub> is not significant in most regions, and there is no significant  
355 difference between the two SRM schemes (Fig. S8S10).

356 The changes in chemical ozone production rates tend to be smaller in the sulfate G4SSA  
357 experiment than in the case of a solar constant reduction in G4SSA-S. There are three possible  
358 factors that contribute to this:

359 1. The entire reaction cycle depends on the availability of sunlight to photolyse O<sub>3</sub> and  
360 NO<sub>2</sub>. Since SRM schemes modulate the intensity of sunlight (here by 1%) reaching the troposphere  
361 in order to mitigate tropospheric warming, this will necessarily also play a role in all changes to  
362 ozone production and loss reactions in our SRM simulations. More importantly, however, the  
363 sulfate injection geoengineering alters stratospheric ozone concentrations, which ultimately  
364 impacts the photochemical environment of the troposphere by changing radiative fluxes into the  
365 troposphere (DeMore et al., 1997; Nowack et al., 2016). For example, a reduced stratospheric  
366 column will help to stimulate the tropospheric photochemistry by allowing more radiation relevant  
367 reactions (1) and (5) to propagate into the troposphere.

368 2. Diffuse radiation under G4SSA promotes the photosynthesis rate and increases canopy  
369 transpiration (Fig. S4). Therefore, we expect that water vapor concentration over the continents

370 with plants would be slightly higher in G4SSA relative to G4SSA-S (Fig. S9S11). Those regions  
371 with higher water vapor (East Asia, South Asia, North America, South Africa) are consistent with  
372 high NO<sub>x</sub> regions (Fig. S10S12). Therefore, the slightly smaller reduction of water vapor under  
373 G4SSA in the regions above increases ozone chemical production compared with G4SSA-S, and  
374 hence G4SSA shows less reduction of ozone chemical production than that in G4SSA-S.

375 3. Different biogenic VOC emissions under G4SSA and G4SSA-S, which, due to their  
376 central role in forming NO<sub>2</sub>, are highly important for ozone production. In both scenarios, lower  
377 temperatures reduce the heat stress on the emitting plants and therefore reduces their VOC  
378 emissions (Tingey et al., 1980; Sharkey and Yeh, 2001; Lathière et al., 2005; Bornman et al., 2015)  
379 (e.g., bio-emitted isoprene, Fig. S11S13). However, at the same time enhanced diffuse radiation  
380 under G4SSA increases biogenic VOC emissions compared with G4SSA-S (Wilton et al., 2011)  
381 (Fig. S11S13i, j, k and l). In Table 1, biogenic VOC-related ozone chemical production is  
382 generally very similar between G4SSA with G4SSA-S (e.g., r-ISOPO<sub>2</sub>-NO, r-MACRO<sub>2</sub>-NO<sub>a</sub>, r-  
383 MCO<sub>3</sub>-NO and r-TERPO<sub>2</sub>-NO), and contributes less than 2% to the overall difference between  
384 G4SSA and G4SSA-S.

### 385 3.3.2 Changes in stratosphere-troposphere exchange

386 Stratospheric chemical and dynamical changes can impact tropospheric ozone not only by  
387 changing the tropospheric photochemical environment, but also by changing the actual transport  
388 of ozone from the stratosphere into the troposphere (Hegglin and Shepherd, 2009; Neu et al., 2014).  
389 This can be either caused by changes in ozone concentrations in the stratosphere, or by changes in  
390 the rate of exchange of air masses between stratosphere and troposphere (i.e., the strength of the  
391 Brewer–Dobson (B-D) circulation and tropopause folds).

392 Fig. 8 shows seasonal latitude-height cross-sections of differences in ozone volume mixing  
393 ratios between G4SSA and RCP6.0 as well as G4SSA-S and RCP6.0 for altitudes above the 500  
394 mb pressure level. Under G4SSA, heterogeneous reactions on the aerosol surfaces lead to  
395 increased halogen activation and with that an enhancement of ozone depletion in mid to high  
396 latitudes (60°-90° N/S in the lower stratosphere (70-150 mb)) (Tilmes et al., 2008, 2009, 2012;  
397 Heckendorn et al., 2009). On the other hand, heterogenous reactions reduce the NO<sub>x</sub> to NO<sub>y</sub> ratio,  
398 which results in an increase in ozone mixing ratios, mainly in the middle stratosphere (10-30 mb)  
399 (Tie and Brasseur, 1995) (Fig. 8a). In addition, changes in stratospheric temperature (warming in  
400 G4SSA and cooling in G4SSA-S) also change the photochemistry of ozone. Altogether, this  
401 results in year-round lower stratospheric ozone loss worldwide that peaks during the return of  
402 sunlight at high SH latitudes- (Fig. S14). In comparison, the solar reduction in G4SSA-S does not  
403 enhance stratospheric heterogeneous reactions. The much smaller change (increase) in ozone (Fig.  
404 8b) is driven by the change of homogeneous chemistry due to slight temperature reduction (Fig.  
405 4b) and). However, in Fig. 4b, there is a slight warming around 50 mb in the slowingtropics, where  
406 ozone concentration also shows a stronger increase (Fig. 8b). As tropospheric cooling results in a  
407 slow-down of the B-D circulation under tropospheric cooling (Fig. 9b) (Lin and Fu, 2013; Nowack  
408 et al., 2015; Shepherd and McLandress, 2011)-, there is an increase of ozone in the tropical  
409 upwelling region, which leads to increasing temperatures there as ozone is a strong shortwave and  
410 longwave absorber. The net result is small ozone increases in the tropical lower stratosphere and  
411 decreases in both extratropical lower stratospheres (Fig. 8b).

412 Age of air is used to indicate the strength of the B-D circulation (Fig. 9). Here, it is  
413 calculated relative to the zonal mean of 1°N at 158.1 mb (Garcia and Randel, 2008; Waugh, 2002).  
414 Older air indicates a slow-down of the B-D circulation. Compared with RCP6.0, both G4SSA and

415 G4SSA-S show older air in the stratosphere indicating a slowdown of the circulation. The cooling  
416 effect in two SRM scenarios correlates with a weakening of tropical upwelling. However, in  
417 G4SSA, the heating of the tropical stratosphere results in enhanced lifting, which counteracts the  
418 weakening of the B-D circulation (Figs. 9a and 9c). Previous studies show controversial results  
419 on how the B-D circulation changes due to extra ~~aerosol~~aerosols in the atmosphere. Aquila et al.  
420 (2012) modeled stronger tropic upwelling after the eruption of Mt. Pinatubo, and other studies also  
421 found enhanced simulated B-D circulation after this volcano eruption (Aquila et al., 2013; Pitari  
422 et al., 2016). The differences between previous studies and our result may be because some  
423 previous studies used fixed ozone, with different stratospheric heating rates. In addition, in  
424 previous studies, the QBO was interactively simulated and the models had a higher model top.  
425 However, with extra black carbon in the stratosphere, the tropical upwelling weakens due to the  
426 simultaneous effect of tropospheric cooling (Shepherd and McLandress, 2011; Mills et al., 2014).  
427 We hope that future studies will address the potential model-dependency of this result.

428 The sum of both effects, stratospheric chemical changes and the impact of B-D circulation  
429 change on STE of ozone, is shown in Fig. 10. In G4SSA, ozone transported from the stratosphere  
430 to the troposphere is significantly decreased by ~25% relative to RCP6.0. In G4SSA-S the  
431 reduction is small. Since the air mass transported from the stratosphere to the troposphere is  
432 reduced in both scenarios, and is even more strongly reduced under G4SSA-S (Fig. 9), we find  
433 that the enhanced stratospheric ozone depletion in G4SSA is the dominant reason for the strong  
434 reduction of STE of ozone. This is also supported by a stratospheric ozone tracer from the model,  
435  $O_3^{\text{Strat}}$ , which is set to ozone mixing ratios in the stratosphere and experiences only chemical loss  
436 in the troposphere without chemical production (Fig. ~~S12~~S15). We thus conclude that the

437 significant changes in STE of ozone in G4SSA are mainly driven by enhanced stratospheric ozone  
438 depletion catalysed through the aerosols (see also Table 1).

### 439 **3.3 Balance of the different mechanisms and uncertainties**

440 In summary, there are two main factors that determine the tropospheric ozone responses in  
441 our SRM and RCP6.0 simulations: (a) changes in tropospheric ozone chemical production/loss  
442 due to water vapor changes and impacts on the photochemical environment of the troposphere as  
443 a result of both changes in stratospheric ozone and (to a smaller degree) the actual dimming of  
444 sunlight depending on the geoengineering scheme, and (b) changes in stratosphere-troposphere  
445 exchange of ozone.

446 These factors can also be used to explain the big picture behind the surface ozone changes  
447 shown in Fig. 7. In G4SSA-S the reduced tropospheric humidity leads to stronger reductions of  
448 ozone loss than the decreases in ozone production, leading to global increases in surface ozone,  
449 but particularly in clean air oceanic environments in the tropics. This net increase in ozone  
450 chemical change is not cancelled out by the slight reduction of ozone transport from the  
451 stratosphere (Fig. 10). In G4SSA, reduction of ozone transport from the stratosphere is the  
452 controlling factor, which overwhelms the increase in net ozone production. The effect is  
453 particularly pronounced at mid-to-high latitudes (Fig. [S12a](#)[S14a](#)), thus giving rise to surface ozone  
454 decreases there (Fig. 7). In contrast, the effect of reduced tropospheric humidity is relatively more  
455 important in the tropics than in other regions, which results in a local increase in surface ozone  
456 under G4SSA. Regionally HO<sub>x</sub>-NO<sub>x</sub> induced reductions in ozone production (Table 1) can  
457 become important to explain surface ozone decreases in NO<sub>x</sub>-polluted land areas in the NH for  
458 both scenarios (Figs. 7 and S6). Further minor contributions to the differences in surface ozone

459 between G4SSA and G4SSA-S are a consequence of changes in water vapor due to regional  
460 canopy transpiration effects and biogenic VOC emissions (e.g., isoprene, Table 1 and Fig. [S44-S13](#)).

461 This study may be biased by the following factors: (1) using prescribed stratospheric  
462 aerosols does not allow the simulation of the full interactions between chemistry, aerosol  
463 microphysics, and dynamics. A fully interactive model including those interactions would be  
464 important. (2) The vertical resolution is not sufficient to produce an interactive QBO in the model  
465 used, which may also affect transport processes. (3) The model does not include the scattering  
466 effect of aerosols on tropospheric photolysis rates, which might lead to an overestimate of the UV  
467 enhancement in the troposphere.

#### 468 **4. Conclusions**

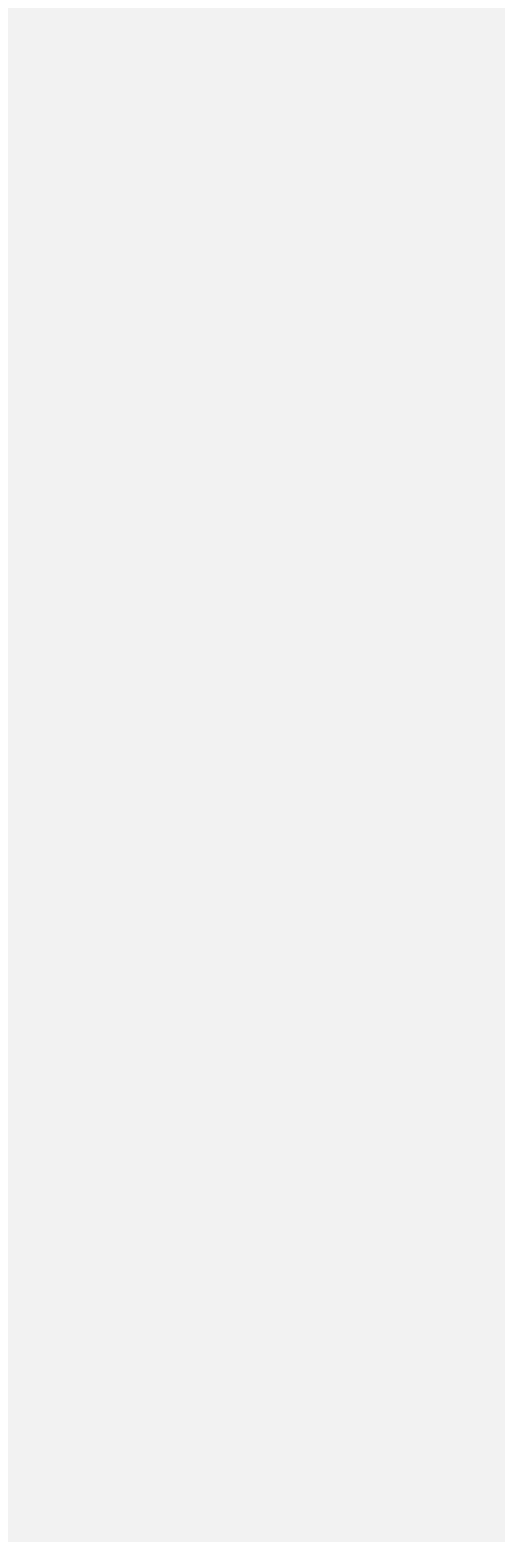
469 Tropospheric ozone changes are to be expected in a geoengineered climate with consequent  
470 impacts on air pollution and crop yields. However, for the scenarios considered here, solar and  
471 sulfate geoengineering could have entirely different impacts, even in terms of the sign of the  
472 response, a rare discrepancy for a surface signal between these two types of geoengineering. There  
473 have been many studies using solar irradiance reductions to illustrate SRM. However, it turns out  
474 that different SRM strategies would have different impacts on hydrology, atmospheric dynamics,  
475 the terrestrial carbon sink, and as investigated in this paper, tropospheric chemistry. These results  
476 also depend on the scenario of future ozone precursor and halogen emissions.

477 We have identified and explained the mechanisms by which stratospheric sulfate  
478 geoengineering would change surface ozone concentrations. We find that geoengineering might  
479 have the potential to significantly reduce some climate impacts, but it cannot fix the problem of  
480 air pollution. To reduce air pollution effectively, changes in surface emissions are key, with  
481 changes in climate (including geoengineering) being only a modulating factor (Monks et al., 2015;

482 Stevenson et al., 2013; Young et al., 2013). More importantly, the surface ozone reduction  
483 between 2030 and 2070 in G4SSA is primarily the result of decreased STE of ozone following  
484 ozone depletion in the stratosphere. The rather mild pollution benefit under the RCP6.0  
485 background would thus be bought at the expense of ~~the~~ delay of ~~the~~ stratospheric ozone recovery,  
486 which would result in enhanced UV penetration to Earth's surface and with that serious impacts  
487 on human health (e.g., skin cancer) and the ecosystem. In the future, potential increases of  
488 stratospheric ozone as a result of geoengineering may result in an increase of surface ozone,  
489 causing more ozone pollution. However, further analysis on air pollutants other than ozone are  
490 needed.

491 As shown by Pitari et al. (2014), impacts on ozone from stratospheric geoengineering can  
492 be highly model dependent. ~~We~~ Therefore, we consider the results here to be a GeoMIP testbed  
493 experiment, and encourage others to compare our results to those from other climate models to  
494 evaluate the robustness of the results presented here.

495  
496 **Acknowledgments.** This work is supported by U.S. National Science Foundation (NSF) grants  
497 AGS-1157525, GEO-1240507, AGS-1430051, and AGS-1617844. Computer simulations were  
498 conducted on the National Center for Atmospheric Research (NCAR) Yellowstone supercomputer.  
499 NCAR is funded by ~~the~~ NSF. The CESM project is supported by ~~the~~ NSF and the Office of  
500 Science (BER) of the US Department of Energy. Peer Nowack is supported by the European  
501 Research Council through the ACCI project, project number 267760. ~~We thank and is now~~  
502 supported through an Imperial College Research Fellowship. We thank Doug Kinnison for helpful  
503 comments and Jean-Francois Lamarque, Daniel Marsh, Andrew Conley, Louisa K. Emmons,  
504 Rolando R. Garcia, Anne K. Smith, and Douglas E. Kinnison for the CAM4-Chem development.



506 **References**

- 507 Ainsworth, E. A., Yendrek, C. R., Sitch, S., Collins, W. J., and Emberson, L. D.: The effects of  
508 tropospheric ozone on net primary productivity and implications for climate change, *Annual*  
509 *Review of Plant Biology*, 63, 637-661, doi:10.1146/annurev-arplant-042110-103829, 2012.
- 510 Ammann, C. M., Washington, W. M., Meehl, G. A., Buja, L., and Teng, H.: Climate engineering  
511 through artificial enhancement of natural forcings: Magnitudes and implied consequences, *J.*  
512 *Geophys. Res.*, 115, D22109, doi:10.1029/2009JD012878, 2010.
- 513 Ashmore, M. R.: Assessing the future global impacts of ozone on vegetation, *Plant, Cell and*  
514 *Environment*, 28, 949-964, doi:10.1111/j.1365-3040.2005.01341.x, 2005.
- 515 Aquila, V., Oman, L. D., Stolarski, R. S., Colarco, P. R., and Newman, P. A.: Dispersion of the  
516 volcanic sulfate cloud from a Mount Pinatubo-like eruption, *J. Geophys. Res.*, 117, D06216,  
517 doi:10.1029/2011JD016968, 2012.
- 518 Aquila, V., Oman, L. D., Stolarski, R. S., Douglass, A. R., and Newman, P. A.: The response of  
519 ozone and nitrogen dioxide to the eruption of Mt. Pinatubo at southern and northern  
520 midlatitudes, *J. Atmos. Sci.*, 70, 894-900, doi:10.1175/JAS-D-12-0143.1, 2013.
- 521 Bala, G., ~~Thompson, S.~~, Duffy, P. B., ~~Caldeira and Taylor, K. and Delire, C.E.~~: Impact of  
522 geoengineering schemes on the ~~terrestrial biosphere~~, *Geophys. Res. Lett.*, ~~29~~global  
523 hydrological cycle, *PNAS*, 105 (22), ~~14-18~~187664-7669, doi:10.~~1029/2002GL015911,~~  
524 ~~20021073/pnas.0711648105.2008.~~
- 525 Bornman, J. F., Barnes, P. W., Robinson, S. A., Ballaré, C. L., Flint, S. D., and Caldwell, M. M.:  
526 Solar ultraviolet radiation and ozone depletion-driven climate change: effects on terrestrial  
527 ecosystems, *Photochem. Photobiol. Sci.*, 14, 88-107, doi:10.1039/C4PP90034K, 2015.
- 528 Chiodo, G., and Polvani, L. M.: Reduction of climate sensitivity of solar forcing due to  
529 stratospheric ozone feedback, *J. Clim.*, 29, 4651-4663, doi: http://dx.doi.org/10.1175/JCLI-  
530 D-15-0721.1, 2015.
- 531 Collines, W. J., Derwent, R. G., Garnier, B., Johnson, C. E., and Sanderson, M. G.: Effect of  
532 stratosphere-troposphere exchange on the future tropospheric ozone trend, *J. Geophys. Res.*,  
533 108 (D12), 8528, doi:10.1029/2002JD002617, 2003.
- 534 Cooper, O. R., et al.: Global distribution and trends of tropospheric ozone: An observation-based  
535 review, *Elementa: Science of the Anthropocene*, 2, 000029,  
536 doi:10.12952/journal.elementa.000029, 2014.
- 537 Crutzen, P.: Albedo enhancement by stratospheric sulfur injections: A contribution to resolve a  
538 policy dilemma? *Climatic Change*, 77(3), 211-220, doi:10.1007/s10584-006-9101-y, 2006.
- 539 DeMore, W. B., Sander, S. P., Golden, D. M., Hampson, R. F., Kurylo, M. J., Howard, C. J.,  
540 Ravishankara, A. R., Kolb, C. E., and Molina, M. J.: Chemical Kinetics and Photochemical  
541 Data for Use in Stratospheric Modeling, Tech. Report, Pasadena, California., 1997.
- 542 Dessler, A. E., and Sherwood, S. C.: A matter of humidity, *Science*, 323, 1020-1021,  
543 doi:10.1126/science.1171264, 2009.
- 544 Emmons, L. K., et al.: Description and evaluation of the Model for Ozone and Related chemical

545 [Tracers, version 4 \(MOZART-4\), Geosci. Model Dev., 3, 43-67, doi:10.5194/gmd-3-43-](#)  
546 [2010, 2010.](#)

547 Fernandez, R. P., Kinnison, D. E., Lamarque, J.-F., Tilmes, S., and Saiz-Lopes, A.: Impact of  
548 biogenic very short-lived bromine on the Antarctic ozone hole during the 21<sup>st</sup> century,  
549 Atmos. Chem. Phys., 17, 1673-1688, doi:10.5194/acp-17-1673-2017, 2017.

550 Ferraro, A. J., Highwood, E. J., and Andrew J Charlton-Perez, A. J.: Weakened tropical  
551 circulation and reduced precipitation in response to geoengineering, Env. Res. Lett., 9,  
552 014001, doi:10.1088/1748-9326/9/1/014001, 2014.

553 Forster, P. et al.: Changes in Atmospheric Constituents and in Radiative Forcing in: Climate  
554 Change 2007: The Physical Science Basis. Contribution of Working Group I to the Fourth  
555 Assessment Report of the Intergovernmental Panel on Climate Change, Cambridge  
556 University Press, Cambridge, United Kingdom and New York, NY, USA, 2007.

557 Garcia, R. R., and Randel, W. J.: Acceleration of the Brewer-Dobson Circulation due to  
558 increases in greenhouse gases, J. Atmos. Sci., 65, 2731-2739, doi:10.1175/2008JAS2712.1,  
559 2008.

560 Govindasamy, B., and Calderia, K.: Geoengineering Earth's radiation balance to mitigate CO<sub>2</sub>-  
561 induced climate change, Geophys. Res. Lett., 27, 2141-2144, doi:10.1029/1999GL006086,  
562 2000.

563 Guenther, A. B., ~~X.~~Jiang, ~~C.-L.~~X., Heald, ~~T.-C.~~L., Sakulyanontvittaya, T., Duhl, ~~L.-K.~~T.,  
564 Emmons, L. K., and ~~X.~~Wang, 2012X.: The Model of Emissions of Gases and Aerosols from  
565 Nature version 2.1 (MEGAN2.1): an extended and updated framework for modeling biogenic  
566 emissions. Geosci. Model Dev., 5, 1471-1492, doi:10.5194/gmd-5-1471-2012, 2012.

567 [Hartmann et al.: Observations: Atmosphere and surface. In: Climate Change 2013: The Physical](#)  
568 [Science Basis. Contribution to Working Group I to the Fifth Assessment Report of the](#)  
569 [Intergovernmental Panel on Climate Change \[Stocker, T. F., Qin, D., Plattner, G.-K.,](#)  
570 [Tignor, M., Allen, S. K., Boschung, J., Nauels, A., Xia, Y., Bex, Y., and Midgley, P. M.](#)  
571 [\(eds\)\]. Cambridge University Press, Cambridge, United Kingdom and New York, NY, USA.](#)

572 Heckendorn, P., Weisenstein, D., Fueglistaler, S., Luo, B. P., Rozanov, E., Schraner, M.,  
573 Thomason, L. W., and Peter, T.: The impact of geoengineering aerosols on stratospheric  
574 temperature and ozone, Environ. Res. Lett., 4, 045108, doi:10.1088/1748-9326/4/4/045108,  
575 2009.

576 Hegglin, M. I. and Shepherd, T. G.: Large climate-induced changes in ultraviolet index and  
577 stratosphere-to-troposphere ozone flux, Nat. Geosci., 2(10), 687-691, doi:10.1038/ngeo604,  
578 2009.

579 Jones, A., Haywood, J., and Boucher, O.: A comparison of the climate impacts of  
580 geoengineering by stratospheric SO<sub>2</sub> injection and by brightening the marine stratocumulus  
581 cloud, Atmos. Sci. Lett., 12, 176-183, doi:10.1002/asl.291, 2011.

582 Kampa, M., and Castanas, E.: Human health effects of air pollution, Environmental Pollution,  
583 151(2), 362-367, doi:10.1016/j.envpol.2007.06.012, 2008.

584 Kinnison, D. E., et al.: Sensitivity of chemical tracers to meteorological parameters in the  
585 MOZART-3 chemical transport model. *J. Geophys. Res.*, 112, D20302,  
586 doi:10.1029/2006JD007879, [20172007](https://doi.org/10.1029/2006JD007879).

587 Lamarque, J.-F., Bond, T. C., Eyring, V., Granier, C., Heil, A., Klimont, Z., Lee, D., Liousse, C.,  
588 Mieville, A., Owen, B., Schultz, M. G., Shindell, D., Smith, S. J., Stehfest, E., Van  
589 Aardenne, J., Cooper, O. R., Kainuma, M., Mahowald, N., Mc-Connell, J. R., Naik, V.,  
590 Riahi, K., and van Vuuren, D. P.: Historical (1850–2000) gridded anthropogenic and biomass  
591 burning emissions of reactive gases and aerosols: methodology and application, *Atmos.*  
592 *Chem. Phys.*, 10, 7017–7039, doi:10.5194/acp-10-7017-2010, 2010.

593 Lamarque, J.-F., Emmons, L. K., Hess, P. G., Kinnison, D. E., Tilmes, S., Vitt, F., Heald, C. L.,  
594 Holland, E. A., Lauritzen, P. H., Neu, J., Orlando, J. J., Rasch, P. J., and Tyndall, G. K.:  
595 CAM-Chem: Description and evaluation of interactive atmospheric chemistry in the  
596 Community Earth System Model, *Geosci. Model Dev.*, 5, 369–411, doi:10.5194/gmd-5-369-  
597 2012, 2012.

598 Lathière, J., Hauglustaine, D. A., De Noblet-Ducoudré, N., Krinner, G., and Folberth, G. A.: Past  
599 and future changes in biogenic volatile organic compound emissions simulated with a global  
600 dynamic vegetation model, *Geophys. Res. Lett.*, 32, L20818, doi:10.1029/2005GL024164,  
601 2005.

602 MacIntosh, C. R., Allan, R. P., Baker, L. H., Bellouin, N., Collins, W., Mousavi, Z., and Shine,  
603 K. P.: Contrasting fast precipitation responses to tropospheric and stratospheric ozone  
604 forcing, *Geophys. Res. Lett.*, 43, 1263–1271, doi:10.1002/2015GL067231, 2016.

605 Mauzerall, D. L., and Wang, X. P.: Protecting agricultural crops from the effects of tropospheric  
606 ozone exposure: Reconciling science and standard setting in the United States, Europe, and  
607 Asia, *Annual Review of Energy and the Environment*, 26, 237–268,  
608 doi:10.1146/annurev.energy.26.1.237, 2001.

609 Meinshausen, M., et al.: The RCP greenhouse gas concentrations and their extension from 1765  
610 to 2300, *Climatic Change*, 109, 213–241, doi:10.1007/s10584-011-0156-z, 2011.

611 Mills, M., Toon, O.B., Lee-Taylor, J., and Robock, A.: Multi-decadal global cooling and  
612 unprecedented ozone loss following a regional nuclear conflict, *Earth's Future*, 2, 161–176,  
613 doi:10.1002/2013EF000205, 2014.

614 Monks, P. S.: Gas-phase radical chemistry in the troposphere., *Chem. Soc. Rev.*, 34(5), 376–395,  
615 doi:10.1039/b307982c, 2005.

616 Monks, P. S., Archibald, A. T., Colette, A., Cooper, O., Coyle, M., Derwent, R., Fowler, D.,  
617 Granier, C., Law, K. S., Mills, G. E., Stevenson, D. S., Tarasova, O., Thouret, V., Von  
618 Schneidmesser, E., Sommariva, R., Wild, O. and Williams, M. L.: Tropospheric ozone and  
619 its precursors from the urban to the global scale from air quality to short-lived climate forcer,  
620 *Atmos. Chem. Phys.*, 15(15), 8889–8973, doi:10.5194/acp-15-8889-2015, 2015.

621 [Morgenstern, L., et al.: Review of the global models used within Phase I of the Chemistry-](#)  
622 [Climate Model Initiative \(CCMI\), \*Geosci. Model Dev.\*, 10,639-671, doi:10.5194/gmd-10-](#)  
623 [639-2017, 2017](#)

624 Neu, J. L., Flury, T., Manney, G. L., Santee, M. L., Livesey, N. J. and Worden, J.: Tropospheric

625 ozone variations governed by changes in stratospheric circulation, *Nat. Geosci.*, 7(5), 340–  
626 344, doi:10.1038/NGEO2138, 2014.

627 Niemeier, U., Schmidt, H., Alterskjær, K., and Kristjánsson, J. E.: Solar irradiance reduction via  
628 climate engineering: Impact of different techniques on the energy balance and the  
629 hydrological cycle, *J. Geophys. Res. Atmos.*, 118, 11,905-11,917,  
630 doi:10.1002/2013JD020445, 2013.

631 [Niemeier, U., and Schmidt, H.: Changing transport processes in the stratosphere by radiative](#)  
632 [heating of sulfate aerosols, \*Atmos. Chem. Phys. Discuss.\*, doi:10.5194/acp-2017-470, 2017.](#)

633 Nowack, P. J., Abraham, N. L., Maycock, A. C., Braesicke, P., Gregory, J. M., Joshi, M. M.,  
634 Osprey, A. and Pyle, J. A.: A large ozone-circulation feedback and its implications for global  
635 warming assessments, *Nat. Clim. Chang.*, 5(1), 41–45, doi:10.1038/nclimate2451, 2015.

636 Nowack, P. J., Abraham, N. L., Braesicke, P. and Pyle, J. A.: Stratospheric ozone changes under  
637 solar geoengineering: implications for UV exposure and air quality, *Atmos. Chem. Phys.*, 16,  
638 4191–4203, doi:10.5194/acpd-15-31973-2015, 2016.

639 Nowack, P. J., Braesicke, P., Abraham, N. L., and Pyle, J. A.: On the role of ozone feedback in  
640 the ENSO amplitude response under global warming, *Geophys. Res. Lett.*, 44,  
641 doi:10.1002/2016GL072418, 2017.

642 Pitari, G., Aquila, V., Kravitz, B., Robock, A., Watanabe, S., Cionni, I., De Luca, N., Genova, G.  
643 I., Mancini, E., and Tilmes, S.: Stratospheric ozone response to sulfate geoengineering:  
644 Results from the Geoengineering Model Intercomparison Project (GeoMIP). *J. Geophys.*  
645 *Res. Atmos.*, 119, 2629-2653, doi:10.1002/2013JD020566, 2014.

646 Pitari, G., Cionni, I., Genova, G. D., Visioni, D., Gandolfi, I., and Mancini, E.: Impact of  
647 stratospheric volcanic aerosols on age-of-air and transport of long lived species, *Atmosphere*,  
648 7 (11), 149, doi:10.3390/atmos7110149, 2016.

649 Portmann, R. W., Solomon, S., Garcia, R. R., Thomason, L. W., Poole, L. R., and McCormick,  
650 M. P.: Role of aerosol variations in anthropogenic ozone depletion in the polar regions, *J.*  
651 *Geophys. Res.*, 101, D17, 22,991-23,006, doi:10.1029/96JD02608, 1996.

652 Rasch, P. J., Crutzen, P. J., and Coleman, D. B.: Exploring the geoengineering of climate using  
653 stratospheric sulfate aerosols: The role of particle size, *J. Geophys. Res.*, 35, L02809,  
654 doi:10.1029/2007GL032179, 2008a.

655 Rasch, P. J., Tilmes, S., Turco, R. P., Robock, A., Oman, L., Chen, C-C., Stenchikov, G. L., and  
656 Garcia, R. R.: An overview of geoengineering of climate using stratospheric sulphate  
657 aerosols, *Phil. Trans. R. Soc. A.*, 366, 4007-4037, doi:10.1098/rsta.2008.0131, 2008b.

658 Robock, A.: Volcanic eruption and climate, *Rev. Geophys.*, 38, 191-219,  
659 doi:10.1029/1998RG000054, 2000.

660 [Sander, S. P., et al.: Chemical Kinetics and Photochemical Data for Use in Atmospheric Studies](#)  
661 [Evaluation Number 17 NASA Panel for Data Evaluation, \*JLP Publ.\*, 10-6, 2011.](#)

662 Sharkey, T. D., and Yeh, S. S.: Isoprene emission from plants. *Ann. Rev. Plant Phys. Plant Mol.*  
663 *Biol.*, 52, 407-436, doi:10.1146/annurev.arplant.52.1.407, 2001.

664 Shepherd, T. G. and McLandress, C.: A Robust Mechanism for Strengthening of the Brewer–  
665 Dobson Circulation in Response to Climate Change: Critical-Layer Control of Subtropical  
666 Wave Breaking, *J. Atmos. Sci.*, 68(4), 784–797, doi:10.1175/2010JAS3608.1, 2011.

667 Silva, R. A., West, J. J., Zhang, Y., Anenberg, S. C., Lamarque, J.-F., Shindell, D. T., Collins,  
668 W. J., Dalsoren, S., Faluvegi, G., Folberth, G., Horowitz, L. W., Nagashima, T., Naik, V.,  
669 Rumbold, S., Skeie, R., Sudo, K., Takemura, T., Bergmann, D., Cameron-Smith, P., Cionni,  
670 I., Doherty, R. M., Eyring, V., Josse, B., MacKenzie, I. A., Plummer, D., Righi, M.,  
671 Stevenson, D. S., Strode, S., Szopa, S. and Zeng, G.: Global premature mortality due to  
672 anthropogenic outdoor air pollution and the contribution of past climate change, *Environ.*  
673 *Res. Lett.*, 8, 34005, doi:10.1088/1748-9326/8/3/034005, 2013.

674 Soden, B. and Held, I.: An Assessment of Climate Feedbacks in Coupled Ocean – Atmosphere  
675 Models, *J. Clim.*, 19(2003), 3354–3360, doi:10.1175/JCLI9028.1, 2006.

676 Solomon, S.: Stratospheric ozone depletion: A review of concepts and history, *Rev. Geophys.*,  
677 37(3), 275–316, doi:10.1029/1999RG900008, 1999.

678 Stevenson, D. S. et al.: Multimodel ensemble simulations of present-day and near-future  
679 tropospheric ozone, *J. Geophys. Res.*, 111, D08301, doi:10.1029/2005JD006338, 2006.

680 Stevenson, D. S., Young, P. J., Naik, V., Lamarque, J. F., Shindell, D. T., Voulgarakis, ~~a~~  
681 Skeie, R. B., Dalsoren, S. B., Myhre, G., Berntsen, T. K., Folberth, G. ~~a~~, Rumbold, S. T.,  
682 Collins, W. J., MacKenzie, I. ~~a~~, Doherty, R. M., Zeng, G., Van Noije, T. P. C., Strunk, a.,  
683 Bergmann, D., Cameron-Smith, P., Plummer, D. ~~a~~, Strode, S. ~~a~~, Horowitz, L., Lee, Y.  
684 H., Szopa, S., Sudo, K., Nagashima, T., Josse, B., Cionni, I., Righi, M., Eyring, V., Conley,  
685 ~~a~~, Bowman, K. W., Wild, O. and Archibald, ~~a~~: Tropospheric ozone changes, radiative  
686 forcing and attribution to emissions in the Atmospheric Chemistry and Climate Model  
687 Intercomparison Project (ACCMIP), *Atmos. Chem. Phys.*, 13(6), 3063–3085,  
688 doi:10.5194/acp-13-3063-2013, 2013.

689 Tang, Q., Hess, P. G., Brown-steiner, B. and Kinnison, D. E.: Tropospheric ozone decrease due  
690 to the Mount Pinatubo eruption : Reduced stratospheric influx, *Geophys. Res. Lett.*  
691 40(July), 5553–5558, doi:10.1002/2013GL056563, 2013.

692 Tie, X., and Brasseur, G.: The response of stratospheric ozone to volcanic eruptions: Sensitivity  
693 to atmospheric chlorine loading, *Geophys. Res. Lett.*, 22, 3035-3038,  
694 doi:10.1029/95GL03057.

695 Tilmes, S., Müller, R., and Salawitch, R.: The sensitivity of polar ozone depletion to proposed  
696 geoengineering schemes, *Science*, 320, 1201-1204, doi:10.1126/science.1153966, 2008.

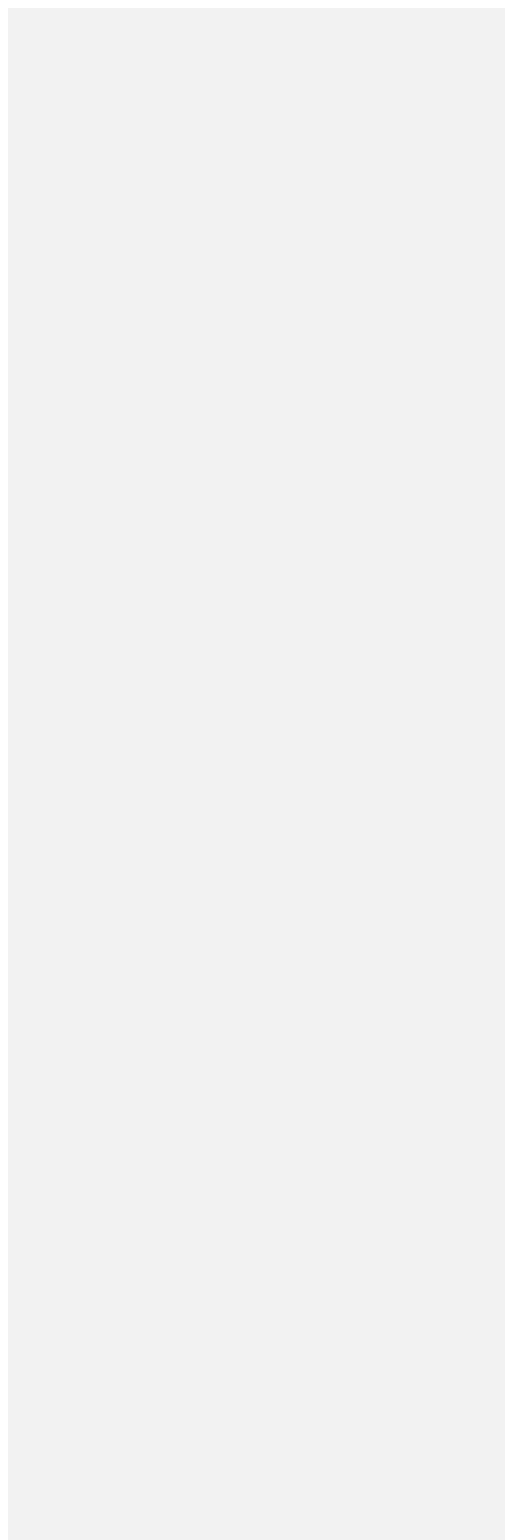
697 Tilmes, S., Garcia, R. R., Kinnison, D. E., Gettelman, A., and Rasch, P. J.: Impact of  
698 geoengineered aerosols on the troposphere and stratosphere, *J. Geophys. Res.*, 114, D12305,  
699 doi:10.1029/2008JD011420, 2009.

700 Tilmes, S., Kinnison, D. E., Garcia, R. R., Salawitch, R., Canty, T., Lee-Taylor, J., Madronich,  
701 S., and Chance, K.: Impact of very short-lived halogens on stratospheric ozone abundance  
702 and UV radiation in a geo-engineered atmosphere, *Atmos. Chem. Phys.*, 12, 10,945-10,955,  
703 doi:10.5194/acp-12-10945-2012, 2012.

- 704 Tilmes, S. et al.: The hydrological impact of geoengineering in the Geoengineering Model  
705 Intercomparison Project (GeoMIP), *J. Geophys. Res. Atmos.*, 118, 11,036-11,058,  
706 doi:10.1002/jgrd.50868, 2013.
- 707 ~~Tilmes, S., et al.: A new Geoengineering Model Intercomparison Project (GeoMIP) experiment~~  
708 ~~designed for climate and chemistry models, *Geosci. Model Dev.*, 8, 43-49, doi:10.5194/gmd-~~  
709 ~~8-43-2015, 2015.~~
- 710 ~~Tilmes, S., Sanderson, B. M., and O'Neill, B. C.: Climate impacts of geoengineering in a~~  
711 ~~delayed mitigation scenario, *Geophys. Res. Lett.*, 43, 8222-8229,~~  
712 ~~doi:10.1002/2016GL070122, 2016a.~~
- 713 Tilmes, S., Lamarque, J-F., Emmons, L. K., Kinnison, D. E., Marsh, D., Garcia, R. R., Smith, A.  
714 K., Neely, R. R., Conley, A., Vitt, F., Val, M. M., Hiroshi, T., Simpson, I., Blake, D. R., and  
715 Blake, N.: Representation of the Community Earth System Model (CESM1) CAM4-chem  
716 within the Chemistry-Climate Model Initiative (CCMI), *Geoscientific Model Development*, 9  
717 (5), 1853-1890, doi:10.5194/gmd-9-1853-2016, 2016b.
- 718 ~~Tilmes, S., et al.: A new Geoengineering Model Intercomparison Project (GeoMIP) experiment~~  
719 ~~designed for climate and chemistry models, *Geosci. Model Dev.*, 8, 43-49, doi:10.5194/gmd-~~  
720 ~~8-43-2015, 2015.~~
- 721 Tingey, D. T., Manning, M., Grothaus, L. C., and Burns, W. F.: Influence of light and  
722 temperature on monoterpene emission rates from Slash Pine. *Plant Physiology*, 65(5), 797-  
723 801, doi: 10.1104/pp.65.5.797, 1980.
- 724 Vingarzan, R.: A review of surface ozone background levels and trends, *Atmos. Env.*, 38, 3431-  
725 3442, doi:10.1016/j.atmosenv.2004.03.030, 2004.
- 726 Waugh, D.: Age of stratospheric air: Theory, observations, and models, *Rev. Geophys.*, 40(4),  
727 doi:10.1029/2000RG000101, 2002.
- 728 Wigley, T. M. L.: A combined mitigation/geoengineering approach to climate stabilization,  
729 *Science*, 314, 452-454, doi:10.1126/science.1131728, 2006.
- 730 Wild, O.: Modelling the global tropospheric ozone budget: exploring the variability in current  
731 models, *Atmos. Chem. Phys.*, 7, 2643-2660, doi:10.5194/acp-7-2643-2007, 2007.
- 732 Wild, O. et al.: Modelling future changes in surface ozone: a parameterized approach, *Atmos.*  
733 *Chem. Phys.*, 12, 2037-2054, doi:10.5194/acp-12-2037-2012, 2012.
- 734 Wilton, D. J., Hewitt, C. N., and Beerling, D. J.: Simulating effect of changes in direct and  
735 diffuse radiation on canopy scale isoprene emissions from vegetation following volcanic  
736 eruptions, *Atmos. Chem. Phys.*, 11, 11723-11731, doi:10.5194/acp-11-11723-2011, 2011.
- 737 Xia, L., Robock, A., Tilmes, S., and Neely III, R. R.: Stratospheric sulfate geoengineering could  
738 enhance the terrestrial photosynthesis rate, *Atmos. Chem. Phys.*, 16, 1479-1489,  
739 doi:10.5194/acp-16-1479-2016, 2016.
- 740 Young, P. J. et al.: Pre-industrial to end 21<sup>st</sup> century projections of tropospheric ozone from the  
741 Atmospheric Chemistry and Climate Model Intercomparison Project (ACCMIP), *Atmos.*  
742 *Chem. Phys.*, 13, 2063-2090, doi:10.5194/acp-13-2063-2013, 2013.

Formatted: Font: Not Bold

Formatted: Font: Times New Roman



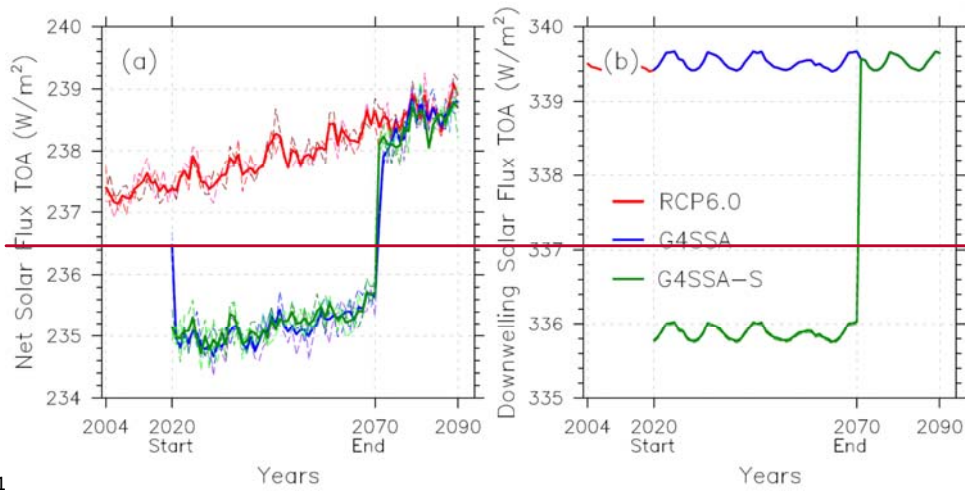
744 **Table 1.** Tropospheric ozone production and loss rates (Tg yr<sup>-1</sup>) over the period of years 2030-  
745 2069 (average of three ensemble members). For chemical ozone production and ozone loss the  
746 net impacts of only the most important reaction pathways are listed.

	RCP6.0	G4SSA	G4SSA-S
O <sub>3</sub> Net Chemical Change	346.1	472.7	384.8
O <sub>3</sub> Tropospheric Dry Deposition	901.5	891.5	909.4
O <sub>3</sub> STE*	555.4	418.8	524.6
O <sub>3</sub> Production	4895.8	4764.0	4671.8
r-NO-HO <sub>2</sub>	3087.3	3031.0	2964.8
r-CH <sub>3</sub> O <sub>2</sub> -NO	1132.3	1105.2	1083.1
r-PO <sub>2</sub> -NO	21.8	20.1	19.9
r-CH <sub>3</sub> CO <sub>3</sub> -NO	183.1	172.2	171.2
r-C <sub>2</sub> H <sub>5</sub> O <sub>2</sub> -NO	6.6	6.7	6.7
0.92*r-ISOPO <sub>2</sub> -NO	149.8	135.3	134.0
r-MACRO <sub>2</sub> -NOa	76.1	69.8	69.5
r-MCO <sub>3</sub> -NO	34.5	30.5	30.3
r-RO <sub>2</sub> -NO	12.2	11.5	11.5
r-XO <sub>2</sub> -NO	66.5	60.8	60.5
0.9*r-TOLO <sub>2</sub> -NO	4.1	4.1	4.1
r-TERPO <sub>2</sub> -NO	18.1	16.9	16.8
0.9*r-ALKO <sub>2</sub> -NO	22.9	23.0	22.9
r-ENE <sub>2</sub> -NO	12.5	11.6	11.7
r-EO <sub>2</sub> -NO	36.8	34.6	34.5
r-MEKO <sub>2</sub> -NO	17.7	17.9	17.8
0.4*r-ONITR-OH	7.5	6.8	6.8
r-jonitr	1.4	1.2	1.2
O <sub>3</sub> Loss	4421.1	4158.6	4151.6
r-O(1D)-H <sub>2</sub> O	2430.4	2286.5	2263.5
r-OH-O <sub>3</sub>	548.2	528.3	527.0
r-HO <sub>2</sub> -O <sub>3</sub>	1288.9	1216.7	1232.9
r-C <sub>3</sub> H <sub>6</sub> -O <sub>3</sub>	13.8	11.5	11.5
0.9*r-ISOP-O <sub>3</sub>	71.4	58.0	57.6
r-C <sub>2</sub> H <sub>4</sub> -O <sub>3</sub>	9.3	7.8	8.0
0.8*r-MVK-O <sub>3</sub>	18.6	15.5	15.7
0.8*r-MACR-O <sub>3</sub>	3.5	2.9	2.9
r-C <sub>10</sub> H <sub>16</sub> -O <sub>3</sub>	37.0	31.5	31.6

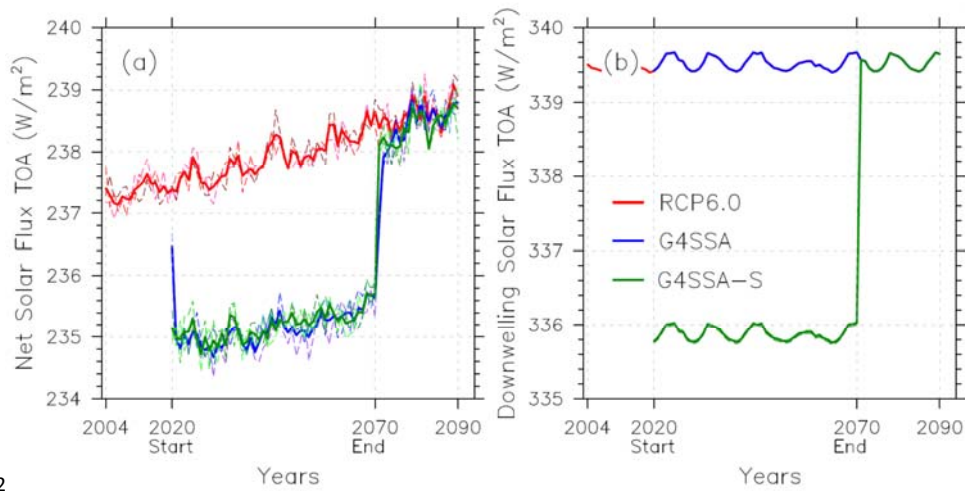
747 \*O<sub>3</sub> STE is ozone transported through the Stratosphere Troposphere Exchange. We calculated  
748 this value using equation –

$$749 \quad O_3 \text{ STE} + O_3 \text{ net tropospheric chemical change} + O_3 \text{ dry tropospheric deposition} = 0$$

750 Tropospheric ozone is defined as ozone concentration less than 150 ppb.

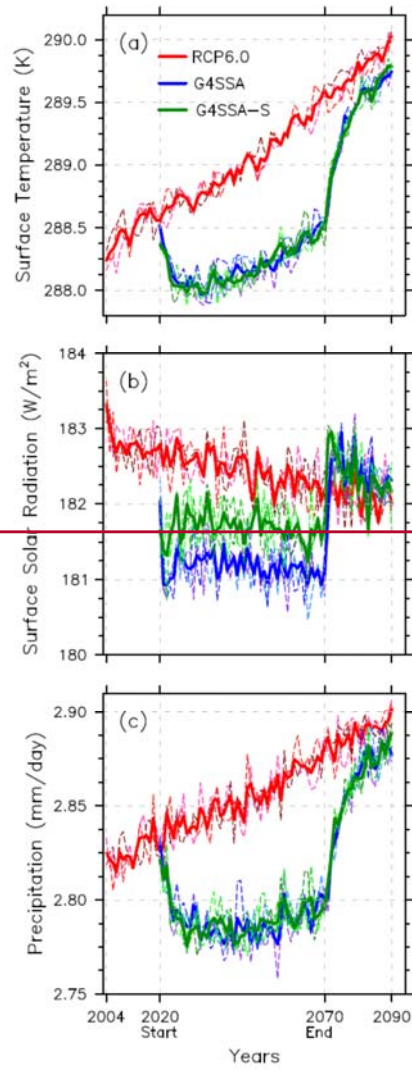


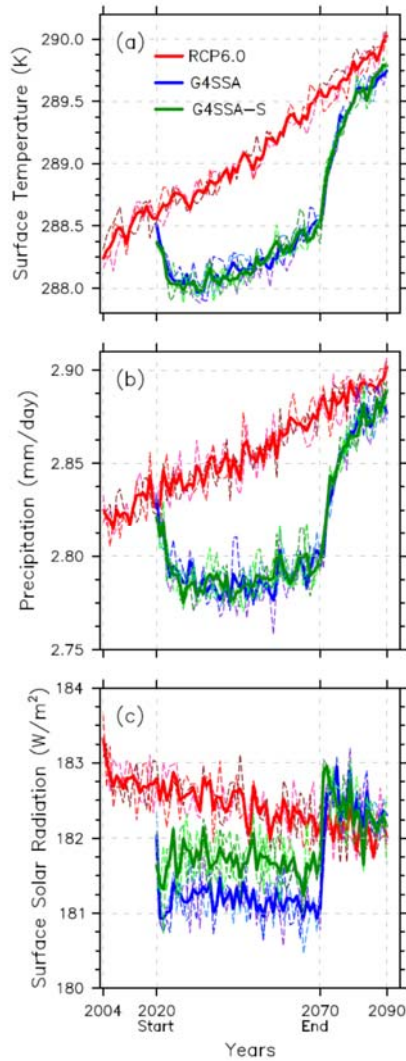
751



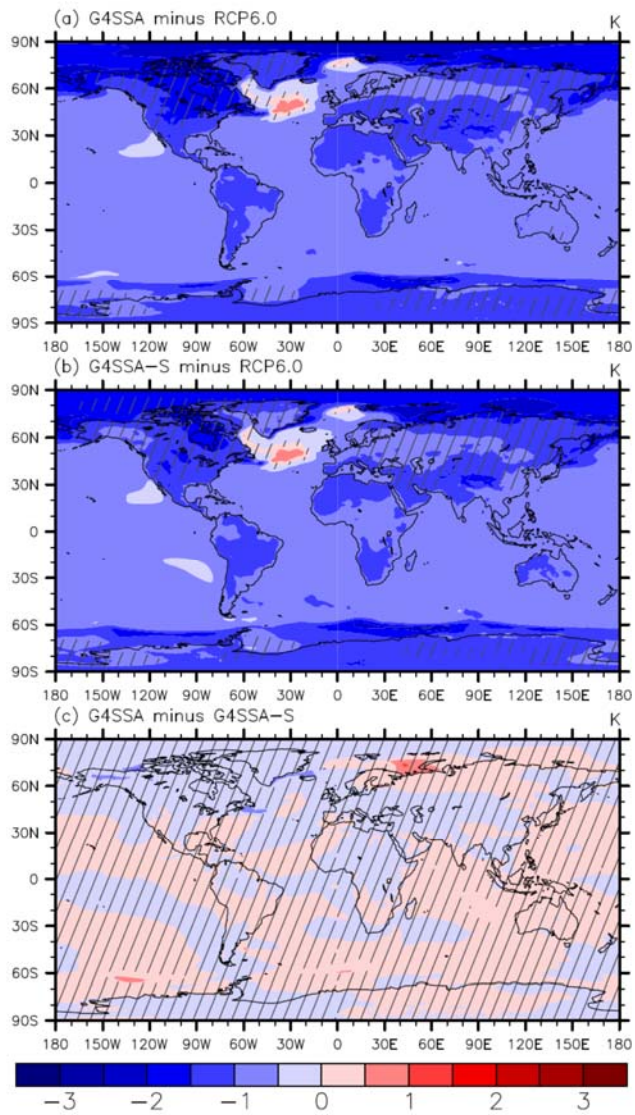
752

753 **Figure 1.** (a) Global averaged annual net solar flux on the top of the atmosphere ( $\text{W}/\text{m}^2$ ) and (b)  
 754 downwelling solar flux on the top of the atmosphere ( $\text{W}/\text{m}^2$ ). Dashed lines are ensemble  
 755 members, and solid lines are the average of three ensemble members. Geoengineering starts at  
 756 January 1<sup>st</sup> 2020 and ends at January 1<sup>st</sup> 2070. The 11-year periodicity is imposed as a prediction  
 757 of the sunspot cycle. In (b) the G4SSA curve exactly covers the RCP6.0 curve.  
 758



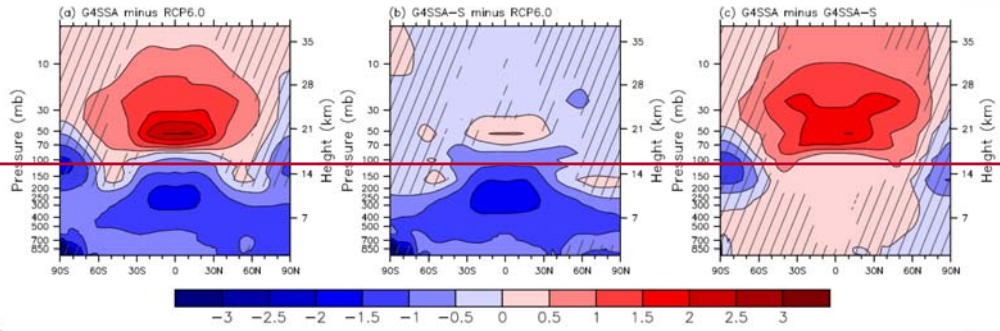


760  
 761 **Figure 2.** (a) Global averaged annual surface air temperature (K), (b) global averaged annual  
 762 precipitation (mm/day), and (c) downwelling surface solar radiation ( $W/m^2$ ), and (c) Land  
 763 average annual canopy transpiration (mm/day). Dashed lines are ensemble members, and solid  
 764 lines are the average of the three ensemble members. Geoengineering starts at 1 January 2020  
 765 and ends at 1 January 2070.



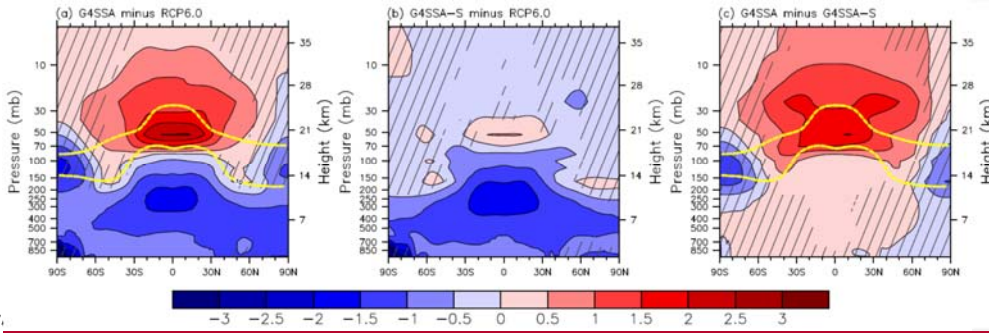
766  
 767 **Figure 3.** Global maps of surface temperature differences (K) between (a) G4SSA and RCP6.0,  
 768 (b) G4SSA-S and RCP6.0, and (c) G4SSA and G4SSA-S over the period 2030-2069. Hatched  
 769 regions are areas with  $p > 0.05$  (where changes are not statistically significant based on a paired  
 770  $t$ -test).

771



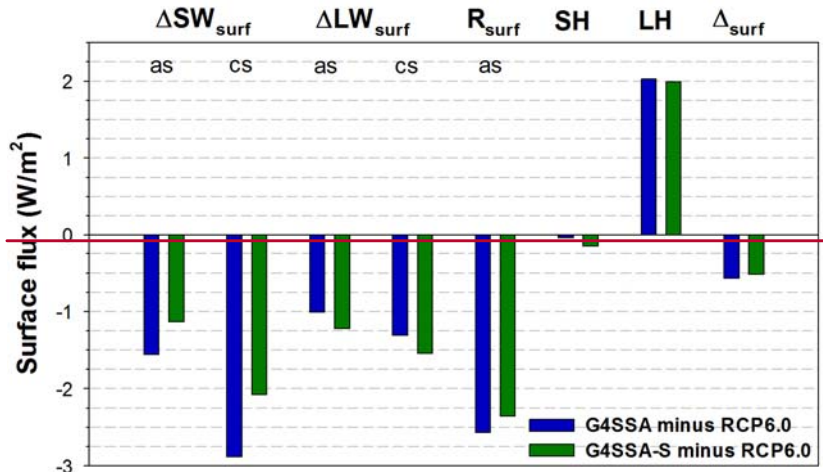
772

773

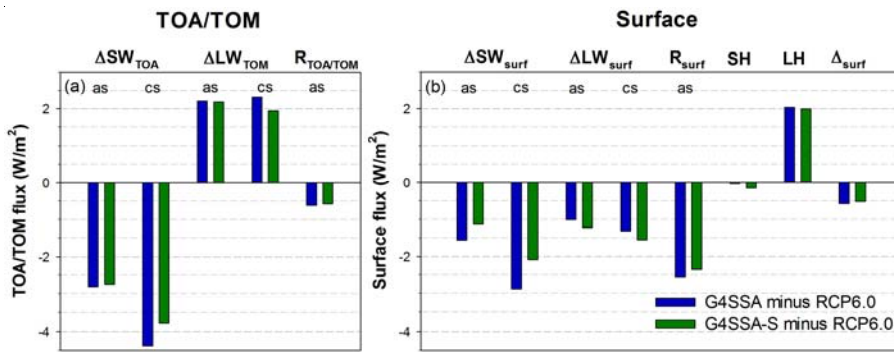


774

775 **Figure 4.** Zonal mean temperature differences (K) in the geoengineering experiments (a)  
776 G4SSA minus RCP6.0, (b) G4SSA-S minus RCP6.0, and (c) G4SSA minus G4SSA-S. These  
777 are averaged for three ensemble members for years 2030-2069. Hatched regions are  
778 insignificant, with  $p > 0.05$ . The yellow dashed lines in (a) and (c) are the injected sulfate aerosol  
779 (surface area density =  $10 \mu\text{m}^2 \text{cm}^{-3}$ ).  
780



781

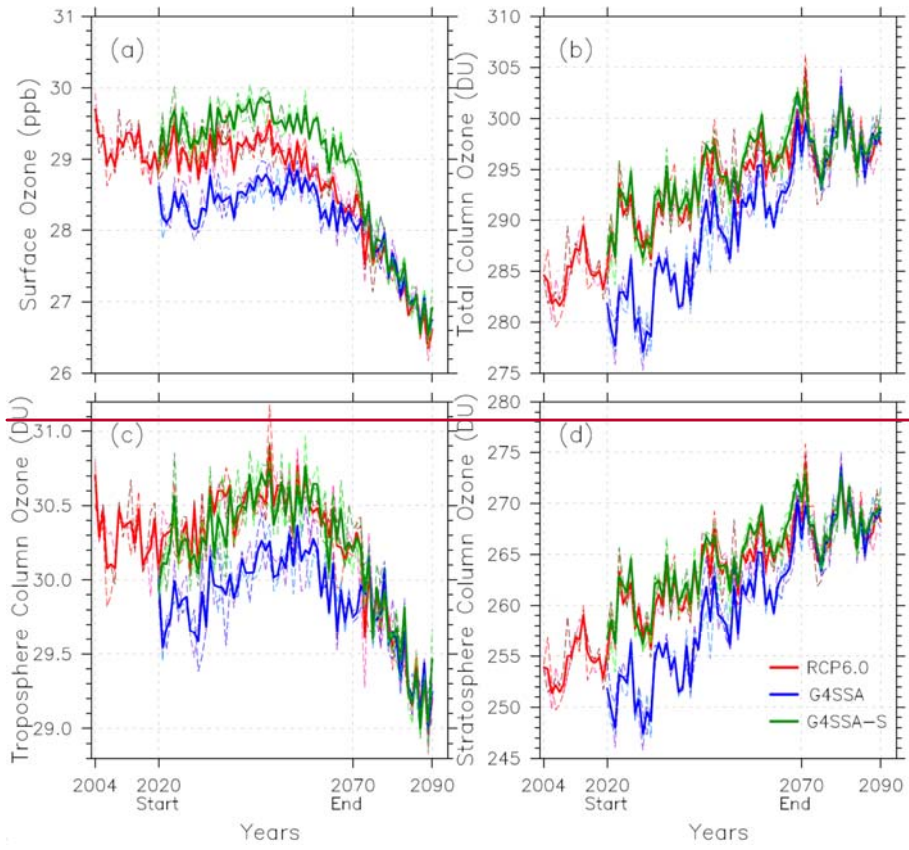


782

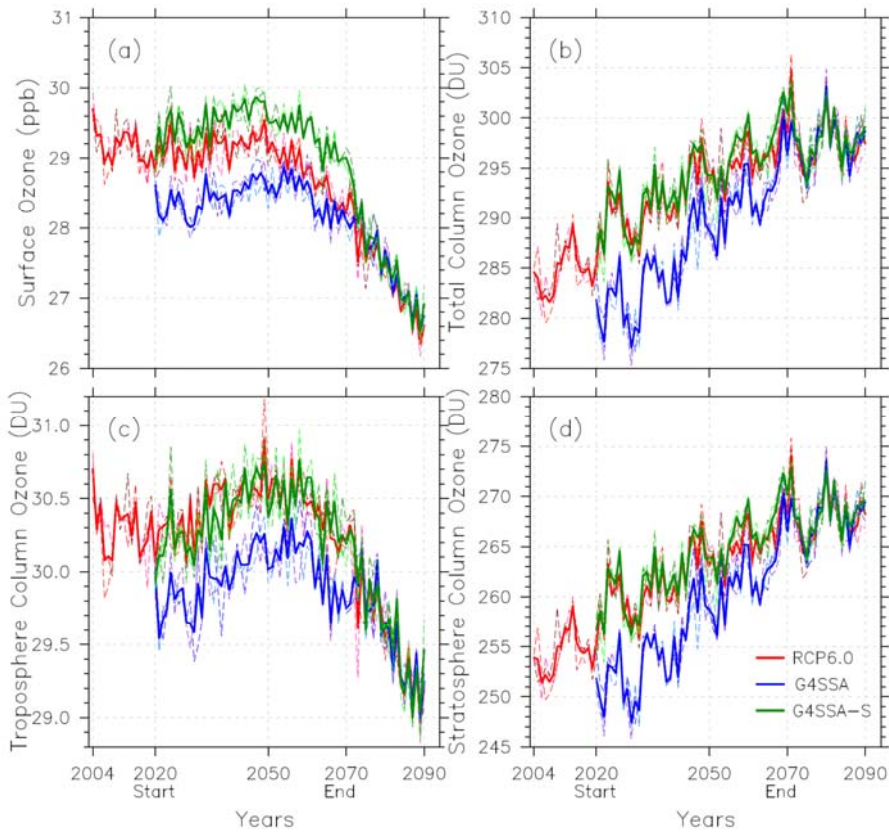
783 **Figure 5.** Energy flux on the top of the atmosphere (TOA) / the top of the model top (TOM) (a)  
 784 and at the surface, (surf) (b), shown as G4SSA minus RCP6.0 and G4SSA-S minus RCP6.0 for  
 785 2030-2069. For all fluxes, downwelling is positive.  $\Delta SW_{surf}$  is the net shortwave flux at the  
 786 surface,  $\Delta LW_{surf}$  is the net longwave flux at the surface,  $R_{surf}$  is the sum of  
 787  $\Delta SW_{surf}$  and  $\Delta LW_{surf}$ , SH is sensible heat, LH is latent heat, and  $\Delta_{surf}$  is the sum of  
 788  $\Delta SW_{surf}$ ,  $\Delta LW_{surf}$ , SH, and LH; as is all sky and cs is clear sky.

789

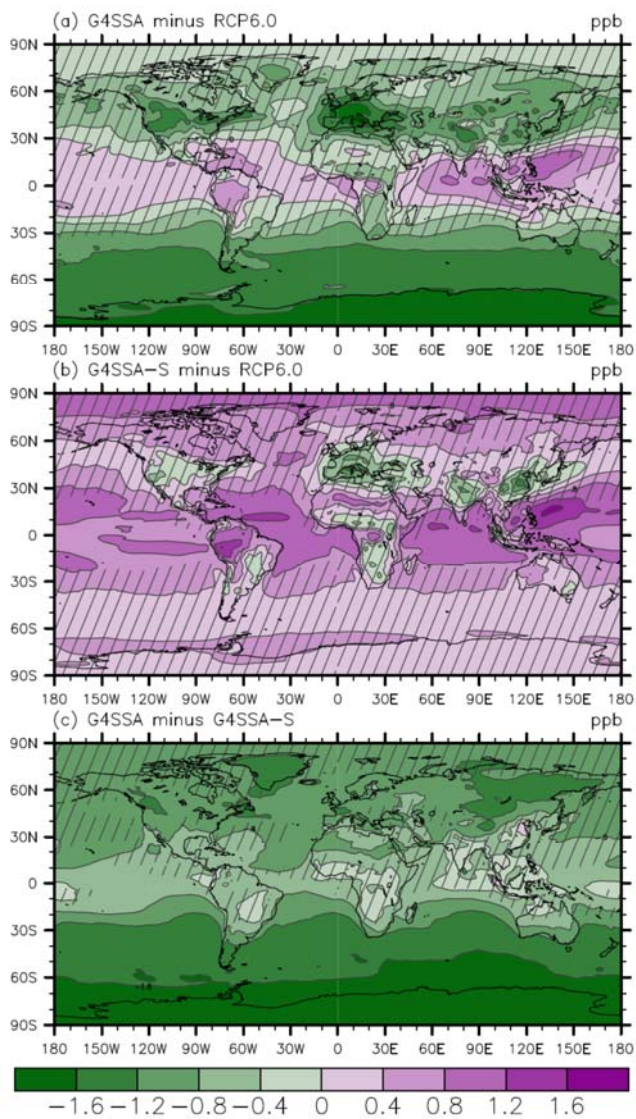
790



791

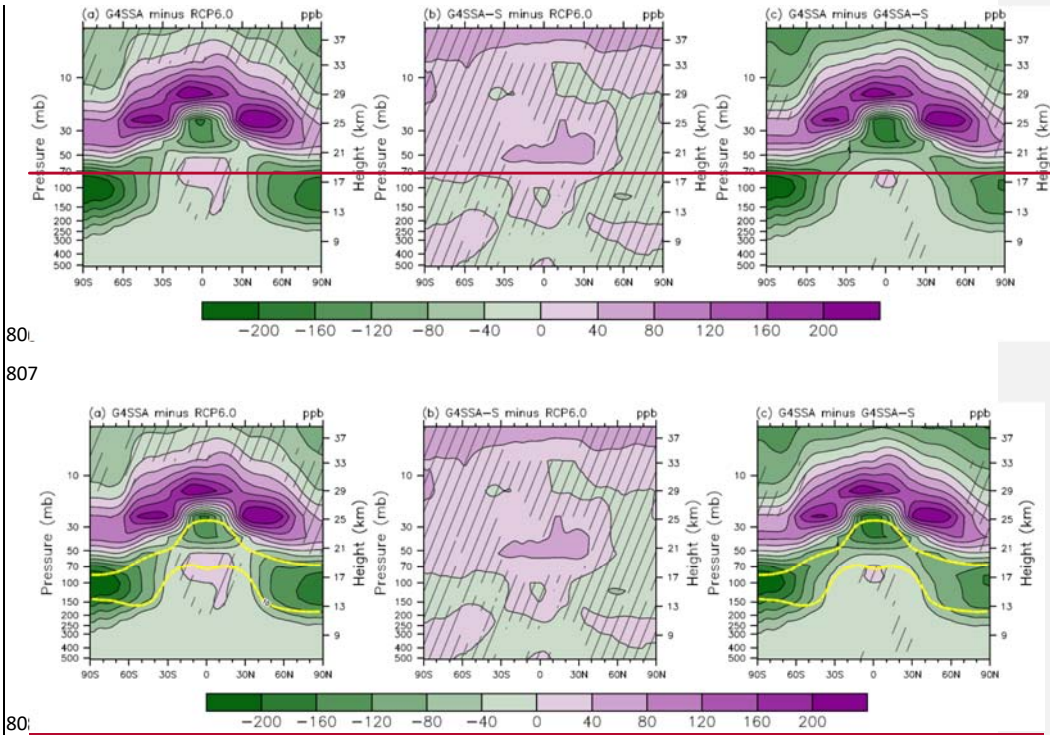


794 **Figure 6.** (a) Global averaged annual surface ozone concentrations (ppb), (b) total column  
 795 ozone (DU), (c) tropospheric column ozone (DU), and (d) stratospheric column ozone (DU).  
 796 Ozone concentration of 150 ppb is used as the boundary of tropospheric ozone and stratospheric  
 797 ozone. Dashed lines are ensemble members, and solid lines are the average of the three  
 798 ensemble members. Geoengineering starts at 1 January 2020 and ends at 1 January 2070.



801

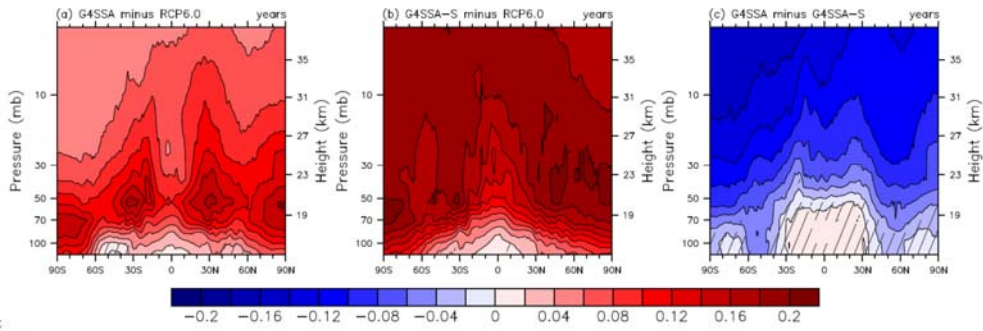
802 **Figure 7.** Global maps of surface ozone concentration differences (ppb) between (a) G4SSA  
 803 and RCP6.0, (b) G4SSA-S and RCP6.0, and (c) G4SSA and G4SSA-S for 2030-2069. Hatched  
 804 regions are insignificant, with  $p > 0.05$ .  
 805



809 **Figure 8.** Zonal mean ozone concentration differences (ppb) in the geoeengineering experiments,  
 810 averaged for three ensemble members for 2030-2069. Hatched regions are insignificant, with  
 811  $p > 0.05$ . The yellow dashed lines in (a) and (c) are the upper and lower limits of the prescribed  
 812 sulfate aerosol (surface area density =  $10 \mu\text{m}^2 \text{cm}^{-3}$ ).

813

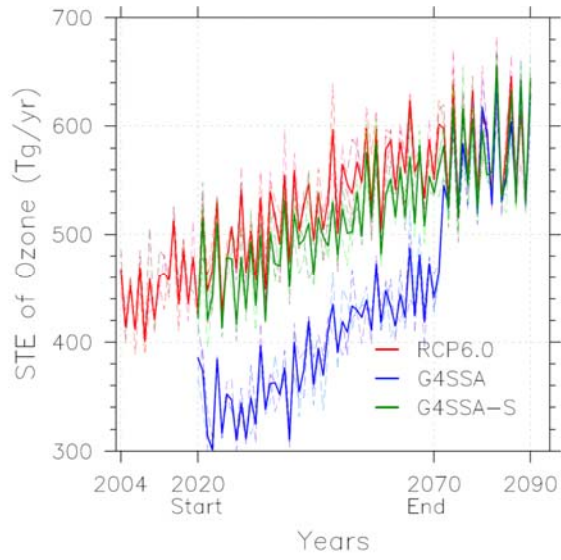
814



815

816 **Figure 9.** Zonal mean age of air differences (years) between (a) G4SSA and RCP6.0, (b)  
817 G4SSA-S and RCP6.0, and (c) G4SSA and G4SSA-S. They are averaged for three ensemble  
818 members for 2030-2069. Hatched regions are insignificant, with  $p > 0.05$ .

819



820

821 **Figure 10.** Global annual averaged ozone transported from the stratosphere to the troposphere  
 822 (STE of ozone) in Tg yr<sup>-1</sup>. Geoengineering starts at 1 January 2020 and ends at 1 January 2070.